A FINAL REPORT TO THE DOE/UCR PROGRAM

TITLE: ELECTROKINETIC DENSIFICATION OF COAL FINES IN WASTE PONDS

DATE: December 18, 1999

PI: E. James Davis (davis@cheme.washington.edu)

STUDENTS: Timothy Johnson, PhD in Chemical Engineering 1999
Gail Furches, Summer Intern 1996 (Murray State University)
Sheryl Filby, Summer Intern 1997 (Gustavus Adolphus College)

INSTITUTION: University of Washington
Department of Chemical Engineering, Box 351750
Seattle, WA 98195-1750
Phone: (206) 543-2250
Fax: (206) 543-3778

GRANT NO.: DE-FG22-95PC95209

PERIOD OF PERFORMANCE: 30 June 1995 to 30 September, 1999

I. ABSTRACT

OBJECTIVE: The objective of this research was to demonstrate that electrokinetics can be used to remove colloidal coal and mineral particles from coal-washing ponds and lakes without the addition of chemical additives such as salts and polymeric flocculants. The specific objectives were:

- Design and develop a scaleable electrophoresis apparatus to clarify suspensions of colloidal coal and clay particles.
- Demonstrate the separation process using polluted waste water from the coal-washing facilities at the coal-fired power plants in Centralia, WA.
- Develop a mathematical model of the process to predict the rate of clarification and the suspension electrical properties needed for scale up.

WORK DONE AND CONCLUSIONS:
It has been demonstrated that heavily contaminated water from a coal-washing facility in Centralia, Washington can be clarified by applying an electric field to the colloidal suspension. The Centralia Mining Company, a subsidiary of PacificCorp, provides coal for two 665 MW coal-burning power plants operated by PacificCorp Power Supply. Water is used to wash the coal during beneficiation to remove fine coal dust and clay particles, and the resulting suspension has a solids content as high as 1%. The colloidal particles typically have mean diameters of 1.8 μm and zeta potentials of ~-25 mV, so electrokinetic treatment is feasible.

The basis of electrokinetic movement of a colloidal particle is that mineral particles such as sand, clay and coal undergo some surface ionization in the presence of water. At the normal pH of water from lakes and rivers the particles become negatively charged. Consequently, they can be moved in an electric field. The counter-ions or cations in the water are attracted to the bound negative charges to produce an electric double layer comprised of bound ions and mobile counter-ions. The electrophoretic motion due to an electric field is retarded by the force exerted on the counter-ions, and in concentrated suspensions additional retardation is caused by particle-particle hydrodynamic interactions. This research examined both the fundamental aspects of the problem and the application to the removal of colloidal coal from polluted water coming from coal-washing facilities.

DISCLAIMER

In the first phase of the work a laboratory test tank was designed, and computerized data acquisition instrumentation and software (Labview) were acquired, programmed and tested. Power supplies and other instrumentation were obtained and installed. Instrumentation for the measurement of particle sedimentation velocities and particle concentrations by light-scattering techniques were designed and built, and measurements of the relevant properties of the water and colloids were made. These included particle zeta potentials, particle sizes and the electrical conductivity of the lake water. A major effort involved the selection and design of the electrodes needed to generate the electrical field, and this was accomplished by using woven sheets of carbon used in the aircraft industry to produce composite polymeric materials. The surface coating of polymeric material was removed to provide inert electrodes that avoid contamination of the process water by the products of electrochemical reaction. The original apparatus was modified to permit hydrogen formed at the cathode (the upper electrode) to be removed to prevent blanketing the electrode surface with a layer of hydrogen. This was accomplished by drilling a series of holes in the cathode and removing the hydrogen from the space above the electrode as shown in Figure 1, a schematic of the apparatus.

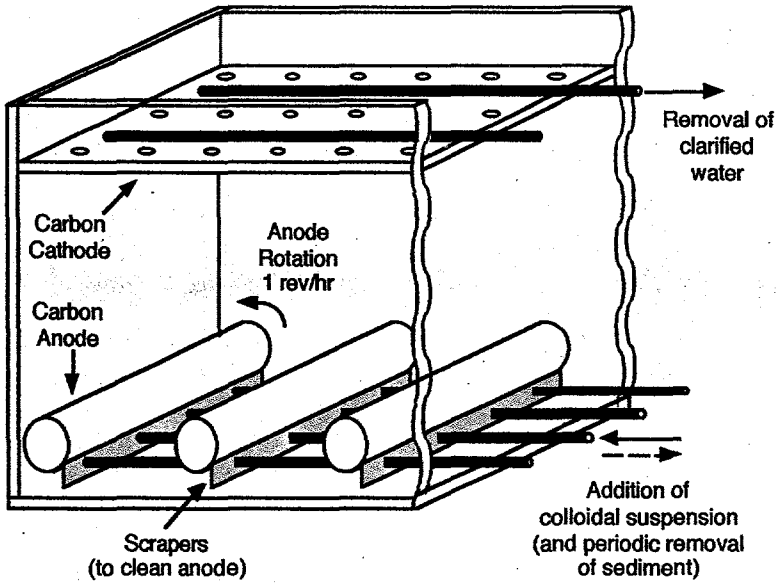

Figure 1. A schematic of the electrophoretic cell.

A series of experiments was carried out to determine the current densities and potentials needed to remove the colloidal particles at an acceptable rate while minimizing gas evolution at the anode and minimizing the power consumption. In addition, studies of the effect of anode rotation on the separation process were carried out, establishing that one revolution per hour was sufficient to keep the electrode clean while not producing convection that would re-suspend the particles. Figure 2 is a photograph of the device that shows the stepper motor and gear train used to rotate the electrodes at any desired speed. It also shows that the distance between the cathode and anode could be adjusted to optimize the performance.

It was found possible to process a highly-contaminated suspension, which had the appearance of black oil, such that after electrokinetic sedimentation no macroscopic particles could be observed in the clarified water. Light scattering was used to detect particles in the suspension, and the light source was a laser beam mounted on one side of the chamber. A detector was mounted on the opposite side to measure the turbidity of the suspension

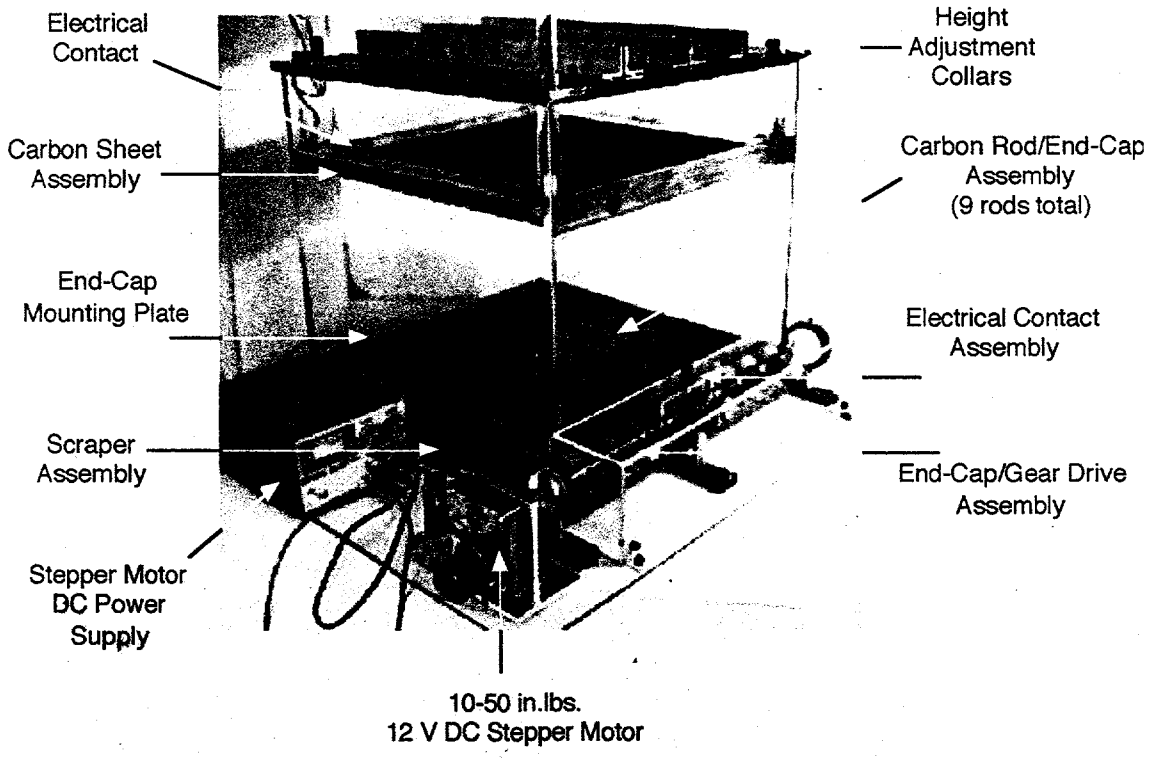

Figure 2. A photograph of the electrophoresis cell.

The separation process is illustrated in Figures 3 and 4. Figure 3 is a frontal view of the chamber when it was loaded with a coal/clay suspension from the Centralia coal-washing facility. The black anode is seen at the base of the suspension, and the suspension was so optically dense that a laser beam could not be passed through it.

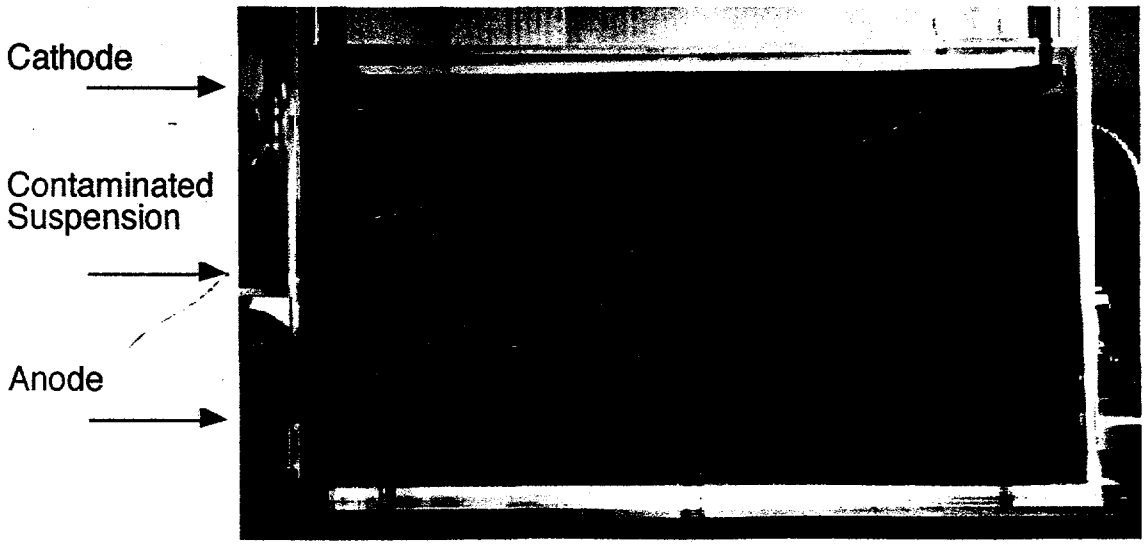

Figure 3. A frontal view of the electrophoretic chamber at the start of a separation process.

Figure 4. A frontal view of the electrophoresis chamber after separation was complete.

Batch operation of the separation system was found to perform very satisfactorily, but continuous or semi-continuous operation is more desirable industrially. It was found that the system could be operated semi-continuously by injecting fresh suspension into the sump below the anode and removing clarified water from above the cathode. In this way the highly concentrated suspension in the sump removed particles from the fresh suspension by agglomeration/coagulation.

Extensive theoretical analysis of the process was carried out, and the results are presented in the reprints provided in the Appendix. It was possible to predict the electrical conductivity of dense suspensions that previous models were not adequate to do.

SIGNIFICANCE TO FOSSIL ENERGY PROGRAM: Coal-washing facilities represent a significant source of water pollution in coal-producing areas. The removal of coal and mineral fines by electrokinetic methods produces clean process water that can be recycled without the addition of flocculating agents, salts and other chemicals. Thus, there is no detriment to wildlife or water supplies if discharged into natural streams or groundwater. The process designed has several advantages including simplicity, potential for scale-up and low power requirements.

II. HIGHLIGHT ACCOMPLISHMENTS

- A novel electrokinetic system has been designed and used successfully to separate colloidal coal/clay particles from process water.
- The apparatus incorporates rotating anodes to prevent fouling and increase the degree and rate of separation.
- The parameters that affect the separation process have been elucidated by experiments and by theoretical modeling of the process. It has been determined that increasing the suspended solids concentration or the electrolyte concentration may decrease power levels, but increases the time necessary for clarification.
- Numerical studies of the hydrodynamics and were performed to predict electrophoretic sedimentation rates and electrical conductivities of dense suspensions.

III. ARTICLES AND PRESENTATIONS

- Two presentations of research results to the scientific staff of PacificCorp Power Supply were made to develop an interaction with the industry.
- Johnson, T.J., Electrokinetic Clarification of Concentrated Colloidal Suspension, Ph.D. Dissertation, University of Washington (1999).
- Johnson, T.J. and Davis, E.J., Electrokinetic Clarification of Colloidal Contaminants, *Environ. Sci. Technol.* **33**:1250-1255 (1999).
- Johnson, T.J. and Davis, E.J., An Analysis of Electrophoresis of Concentrated Suspensions of Colloidal Particles, *J. Colloid Interface Sci.* 215:397-408 (1999).
- Johnson, T.J. and Davis, E.J. Experimental Data and Theoretical Predictions for the Rate of Electrophoretic Clarification of Colloidal Suspensions, *Environ. Sci. Technol.* , submitted for pulication and under revision (1999).

IV. APPENDIX

The appendix consists of reprints of the published work.

Environ. Sci. Technol. 1999, 33, 1250–1255

Electrokinetic Clarification of Colloidal Suspensions

TIMOTHY J. JOHNSON AND
E. JAMES DAVIS*

Department of Chemical Engineering, Box 351750, University of Washington, Seattle, Washington 98195-1750

A novel apparatus has been developed for the electrophoretic clarification of concentrated colloidal suspensions. The laboratory equipment is capable of being scaled up to much larger capacity. The apparatus was designed to process suspensions in either batch or semicontinuous operation, and it has been used to demonstrate the removal of coal/clay colloidal matter from the effluent of a coal-washing facility. In addition, a parametric study of sodium–bentonite suspensions in batch operation was performed to elucidate the effects of initial colloid and electrolyte (NaCl) concentrations on the rate of clarification and the instantaneous power requirements. It was found that an increase in either the initial particle or electrolyte concentration (up to 50 mg of NaCl/L) caused a decrease in the instantaneous power levels but increased the time necessary to reach a given solution clarification. Typical electrophoretic clarification experiments resulted in 99.9% removal of the colloidal matter. In semicontinuous operation it was shown that a 0.2 wt % sodium–bentonite suspension could be clarified to 2.6×10^{-4} wt % in 13.5 h without the addition of flocculants or other chemicals.

Introduction

A significant problem in the preparation of coal for coal-fired power plants is the production of a polydisperse, colloidally contaminated aqueous suspension of coal and clay produced by coal washing. Due to the surface charge and the small size of the particles, a stable colloidal suspension is formed which will not undergo gravitational sedimentation at acceptable rates. The consolidation technique which is most often used for treating the effluent from coal washing and other contaminated streams is the addition of high molecular weight polyelectrolytes or other chemical additives. Grant et al. (*1*) used a surfactant (sodium dodecyl sulfate or cetyltrimethylammonium bromide) and found that the rate and extent of dewatering of iron oxide fines increased with increasing surfactant concentration. However, clarification via surfactant or polyelectrolyte addition can be expensive, and one must also be concerned about discharging the treated fluid to the environment after it has been chemically altered.

An alternative clarification technique, which has been known for several decades, and which is chemically non-invasive, and possibly less costly, is the application of an electric field to the colloidal suspension. When an electric field is applied to the suspension, the particles will move in the direction of the electric field lines. This phenomenon of particle movement relative to the surrounding stagnant fluid, due to an applied electric field, is known as *electrophoresis* and results from the fact that the colloidal particles become charged in water at the typical pH's encountered. In 1809 Reuss (*2*) observed this phenomena and the related phenomenon of *electroosmosis* in which the fluid moves through a stationary porous medium due to the applied electric field.

Since the 1930s electrokinetic phenomena have been applied to various processes ranging from the separation of proteins (*3*) to the stabilization of soft soils (*4*). In the 1960s Sprute and Kelsh (*5*) at the Bureau of Mines began to investigate the use of electrokinetics for the densification of mill tailings and coal-processing waste. Stanczyk and Feld (*6*), also at the Bureau of Mines, investigated electrokinetics for dewatering phosphate clays.

Since the Bureau of Mines investigations, several other researchers have tried to incorporate electrokinetics as a separation technique. Lockhart (*7*) was able to clarify clay suspensions and mine tailings, Wilmans and Van Deventer (*8*) treated kimberlite slimes from diamond mining, and Yoshida et al. (*9*) treated bentonite sludge. Sauer and Davis (*10*) were able to remove fine particles of coal and clay from the water of a coal-washing waste pond using a small laboratory apparatus. They determined that the electric field does not need to be applied throughout the entire course of the electrokinetic processing, thus lowering the costs associated with power consumption. Shang and Lo (*11*) made further improvements in reducing the power consumption of electrokinetic techniques in their investigation of the consolidation and dewatering of a phosphate clay suspension from a waste disposal pond. They showed that the efficiency of electrokinetic treatment was improved when the current was applied in cycles of 15 min ON and 5 min OFF, a 25% reduction in power consumption. Electrophoresis has also been applied to colloidal suspensions in nonaqueous media. Shih et al. (*12*) investigated the sedimentation of illite particles in toluene containing asphaltene, Lee et al. (*13*) studied the rate of sedimentation of α-alumina particles in xylene for various concentrations of a surfactant which controlled the surface charge on the particles, and Matsumoto et al. (*14*) removed oxidized aluminum and iron particles from kerosene.

Successful laboratory studies have not yet led to widespread commercial application. This can be partly attributed to the low rates of particle migration in an electric field and partly to a poor understanding of particle motion in concentrated suspensions when an electric field is applied. The latter issue makes it difficult to scale-up results from the laboratory to commercial sizes.

Numerous analyses of single particle motion in an electric field have been published. The first analysis of electrophoretic motion was that of Smoluchowski (*15*) for a single sphere with a low surface potential and a nonpolarizable thin electric double layer moving in an infinite surrounding fluid. Smoluchowski obtained the particle mobility, U_e, given by

$$U_e = \frac{v_e}{E} = \frac{\epsilon_0 \epsilon_r}{\mu} \zeta \qquad (1)$$

in which v_e is the velocity of the particle in the stagnant fluid due to the applied electric field E, ϵ_0 is the permittivity of free space, ϵ_r is the dielectric constant of the surrounding fluid, μ is the viscosity of the fluid, and ζ is the zeta potential. The zeta potential must be less than $|\pm 25|$ mV for eq 1 to be valid.

A measure of the thickness of the electric double layer is given by κ^{-1}, where κ is the Debye–Hückel parameter. The

* Corresponding author phone: (206) 543-0298; fax: (206) 543-3778; e-mail: davis@cheme.washington.edu.

10.1021/es980835y CCC: $18.00
Published on Web 02/27/1999

TABLE 1. Summary of Colloidal Suspension Characteristics

	suspension	
	coal-washing[a]	sodium–bentonite[b]
vol av diam (μm)	1.07	3.0
specific gravity of particles	1.2	2.5
solids content (wt %)	0.2	0.2–0.3
electrophoretic mobility ($m^2/V-s$)	-3.2×10^{-8}	$-(2.15 \text{ to } 2.28) \times 10^{-8}$
initial pH of suspension	8.2	9.0
suspension conductivity (mS/m)	385.7	71.4–153.1

[a] Coal-washing suspension from Centralia Mining Co., Centralia, WA. [b] Sodium–bentonite particles from Whittaker, Clark, and Daniels, Inc.

Debye–Hückel parameter is a function of the concentration of ionic species, C_i^∞, in the bulk solution, and the valence of the ions present, z_i; that is

$$\kappa = \left(\frac{F^2 \sum_i C_i^\infty z_i^2}{\epsilon_0 \epsilon_r RT}\right)^{1/2} \quad (2)$$

Here F is the Faraday constant, R is the gas constant, and T is the absolute temperature. A thin electric double layer corresponds to large κa ($\kappa a > 100$), where a is the particle radius.

In an attempt to relax the restrictions in the Smoluchowski theory, Kozak and Davis (*16*) obtained an analytical solution for the electrophoretic mobility of a concentrated suspension of particles with a moderately thin and polarizable electric double layer ($\kappa a > 50$) in a single z–z electrolyte solution. The distortion of the electric double layer is referred to as the relaxation effect and has been shown to be small for large κa ($\kappa a \geq 100$ for $|\zeta| \geq 100$ mV) or for small zeta potentials ($|\zeta| \leq 50$ mV when $\kappa a \approx 10$) (*17, 18*). By including the relaxation effect, Kozak and Davis obtained the solution

$$U_e = \frac{\epsilon_0 \epsilon_r}{\mu} \zeta - \frac{2\epsilon_0 \epsilon_r KRT}{\mu z F (1 + K)} \Lambda_{2,0} \quad (3)$$

in which $\Lambda_{2,0}$ is defined by

$$\Lambda_{2,0} = \ln\left[\frac{1 + \exp(F|z\zeta|/2RT)}{2}\right] \quad (4)$$

The function K depends on the solids volume fraction, ϕ, and the diffusivity, D_-, of the anionic species (for $\zeta > 0$) and is

$$K = \frac{2(1 + 2\phi)}{\kappa a (1 - \phi)} \left(1 + \frac{4C_\infty RT}{\mu D_- \kappa^2}\right) \exp\left(\frac{F|z\zeta|}{2RT}\right) \quad (5)$$

For $\zeta < 0$, D_- should be replaced by D_+, the diffusion coefficient of the cationic species. The first term on the right side of eq 3 is Smoluchowski's result, and the second term accounts for particle–particle interactions, electric field retardation due to the relaxation effect, and other electric double-layer effects. Hydrodynamic interactions and electric double-layer effects reduce the mobility of the particles compared to the mobility determined with Smoluchowski's theory. Kozak and Davis (*19*) later extended their analysis to suspensions of colloidal particles with moderately thick electrical double layers ($\kappa a > 20$).

Despite the multiple factors that decrease the electrophoretic mobility, electrokinetic clarification techniques are still a viable alternative for colloidal solutions which can be treated over long periods of time, for example, the removal of colloidal contaminants from settling ponds and lakes. This paper focuses on a new electrophoretic apparatus which can process concentrated colloidal suspensions on either a batch or semicontinuous basis for application in which chemical alteration of the suspension is undesirable and where low clarification rates of the suspension are acceptable.

Colloid Properties

The colloidal suspensions studied were analyzed for electrical conductivity, particle size, and average electrophoretic mobility. The conductivities of the colloidal suspensions were determined by a Jenway 4320 conductivity meter. The volume average diameters of the particles were determined using a Horiba Model CAPA-500 centrifugal particle analyzer. By measuring the sedimentation rate by light transmission, the particle diameter can be determined from Stokes' centrifugal sedimentation equation. The electrophoretic mobility was determined using a Rank Brothers Mark II microelectrophoresis apparatus. The average electrophoretic mobility was taken to be the average of 20 measurements for a particular suspension. A summary of the characteristics of the suspensions is provided in Table 1.

The colloidal suspension of principal concern here is wastewater containing coal and clay colloids obtained from the coal-washing effluent at the Centralia Mining Co. located in Centralia, WA. This suspension contained particles with a volume average diameter of 1.07 μm and a solids content of 0.2 wt % of which approximately 64% was clay. The average electrophoretic mobility was found to be -3.2×10^{-8} $m^2/(V \cdot s)$. The suspensions introduced into the experimental apparatus exhibited no gravitational sedimentation and no flocculation in the absence of an electric field.

Since the colloidal matter was more clay than coal and since the effluent varied from day-to-day, separate experiments were performed using a well-characterized clay. The clay used as the model colloid suspension was montmorillonite (sodium–bentonite) obtained from Whittaker, Clark, and Daniels, Inc. No purification of the montmorillonite was performed. The montmorillonite came as a dry powder and was later suspended in reverse osmosis (RO) treated water as needed for the experiments. To obtain a fine dispersion of particles, the water was stirred with a magnetic stirrer while the clay was added slowly to prevent clumping. The suspension was then stirred for an additional 10 min to ensure a homogeneous suspension of particles. The volume average diameter of the particles was found to be 3.0 μm.

The experiments conducted with the montmorillonite varied in initial clay concentration and initial salt (NaCl) concentration in the aqueous solution. Two clay concentrations were investigated, 0.2 and 0.3 wt %, because these concentrations were similar to the coal-washing effluent studied. For these clay concentrations, the average electrophoretic mobility and conductivity were measured as a function of salt concentration (0, 25, 50, and 100 mg/L), and the results are presented in Figure 1a,b, respectively. For the 0.2 wt % suspension the pH varied from 9.1 to 8.5 for a NaCl concentration of 0 and 100 mg/L, respectively. For the 0.3 wt % suspension the pH varied from 9.4 to 8.8 for a NaCl concentration of 0 and 100 mg/L, respectively. The literature reports spontaneous flocculation for montmorillonite when the pH is less than 3.5 (*20*) and a critical coagulation

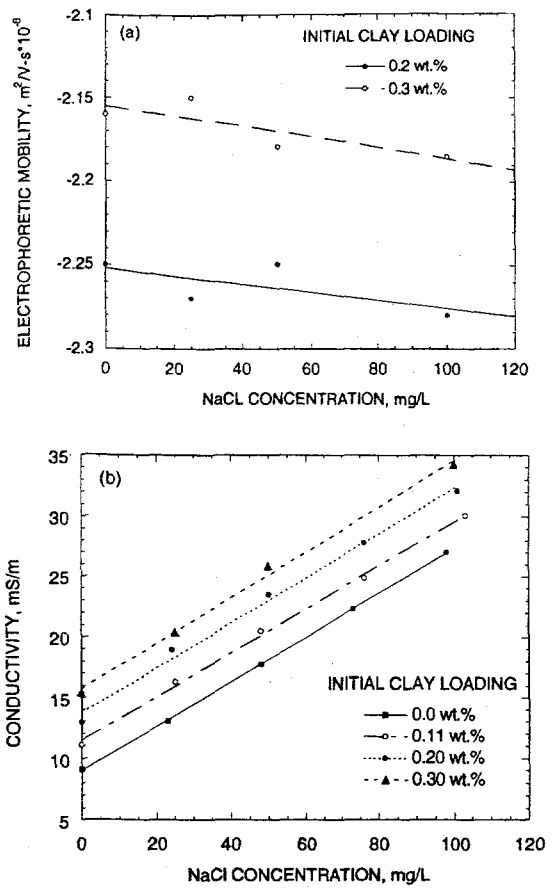

FIGURE 1. (a) Effects of NaCl concentration on the electrophoretic mobility of the sodium–bentonite colloid particles and (b) the effects of sodium–bentonite and NaCl concentrations on the conductivity of the colloidal suspension.

concentration (ccc) for a $|z| = 1$ electrolyte of 0.008 ± 0.006 mol/L (*21*). The pH values and the electrolyte concentrations used throughout these experiments never exceed these limits. Although the 100 mg/L (0.017 mol/L) concentration of NaCl is close to the lower limit of the reported ccc, no appreciable flocculation appeared to occur within 72 h in the absence of the applied electric field.

Experimental Apparatus

A benchtop electrophoretic apparatus was designed and constructed with industrial applications and scalability in mind. The apparatus, shown in Figure 2, consisted of a cubic acrylic tank with inner dimensions of 36.8 × 36.8 × 36.8 cm. The top electrode was a 0.64 cm thick carbon sheet with dimensions 36.3 × 33.3 cm. Because hydrogen gas is produced at this cathode by electrolysis of water, a number of 0.64 cm diameter holes were drilled through the carbon sheet to facilitate the escape of hydrogen gas. In the absence of these holes a layer of hydrogen formed at the lower surface, blanketing the electrode and preventing contact with the electrolyte solution. The cathode could be positioned at any height within the tank.

The anode was a series of nine 2.54 cm diameter solid carbon rods centered 3.8 cm above the bottom of the tank. The carbon electrodes were obtained from Graphite Sales, Inc. The carbon rods were designed to be rotated to clean the electrodes as the experiment proceeded. To do this, a shaft was extended from the end of each carbon rod through the tank wall. On each shaft a 24-pitch bronze worm gear was placed. The pitch diameter was 2.12 cm. A steel shaft with nine, appropriately placed, 24-pitch steel worms meshed

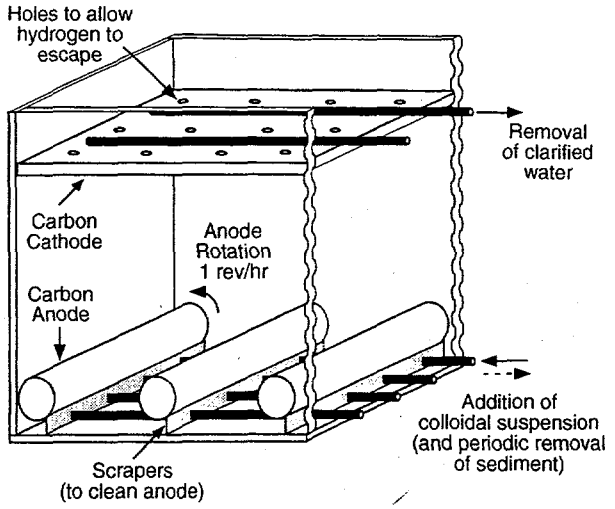

FIGURE 2. Experimental electrophoresis apparatus.

with the bronze worm gears. The pitch diameter of these worms was 1.27 cm. The steel shaft was rotated by means of a 10–50 in.-lbs 12 V DC stepper motor. The power supply for the stepper motor was a Hewlett-Packard 6218C DC supply. As the carbon rods rotated they were cleaned by coming into contact with a flexible plastic scraper which touched the bottom of each carbon rod.

The power supply connected to the electrodes was a Hewlett-Packard 6555A DC supply. The connection to the nine carbon rods was made by contacting a lead from the positive terminal of the power supply to the steel shaft on which were mounted the nine steel worms. The charge was then transferred to the bronze worm gears and then through a wire running from the bronze gear through the shaft in the tank wall and finally to the carbon rods.

For the semicontinuous electrophoretic experiments a fresh colloidal suspension was added in the sump below the carbon rods while the clarified water was removed from the space above the carbon sheet. The addition and removal of solution was done by a Masterflex peristaltic pump with two pump heads, one pump head for the colloidal input tube and one pump head for the clarified solution output tube. To evenly distribute the addition of the colloid suspension, the input tube from the first pump head was split into four 0.64 cm i.d. Tygon tubes which were placed in the sump. Each of the four tubes had 1.0 mm holes drilled every 3.8 cm along the axis of the tube for the addition of the colloidal suspension. The clarified solution was extracted through two 0.64 cm i.d. Tygon tubes with 1.0 mm diameter holes drilled every 3.8 cm. These two output tubes were then connected to a single tube which led to the appropriate pump head.

As the particles settled due to the electric field, a clear zone formed above the sedimenting clay particles. To determine the final weight percent of particles remaining in the clear zone, an optical system based on turbidity was setup. The light source was a 20 mW HeNe laser, and the detector was a Newport Research Model 815 photosensor connected to a Newport Research Model 815 power meter. The laser and the photosensor were placed on opposite sides of the apparatus at a height which was the midpoint between the top and bottom electrodes. Upon calibration, the power meter readings could be directly correlated to the solids content of the clarified solution at this point. Although a concentration gradient of particles exists during the clarification process, it is assumed that the solids content at the midpoint adequately represents the solids content of the bulk clarified solution after long times.

Sedimentation Experiments

The electrophoresis apparatus was filled with the suspension to be studied. The electric field was then applied as soon as any observable convective motion ceased. The experiments were performed under constant current conditions (100 mA or 0.827 A/m^2) with the carbon cathode located 14 cm above the top of the carbon rods. With this electrode configuration, the test volume was 24 L. The maximum current density of 0.827 A/m^2 was chosen because at higher current densities the generation of oxygen at the anode due to electrolysis was excessive and caused convective mixing of the colloidal suspension as bubbles rose through the suspension. The suspensions to be studied contained either the coal-washing wastewater or the model montmorillonite colloidal suspension with various particle and/or salt concentrations.

Effects of Anode Surface Cleaning. To ensure that the rotating anode rods did not hinder the rate of clarification, two experiments were performed with a 0.2 wt % montmorillonite suspension in RO water. In one experiment, the carbon rods were rotated at a slow rate (1 revolution/h) to minimize convective motion within the apparatus. In the other experiment, the carbon rods remained stationary. There appeared to be a slight advantage in the rate of clarification when the rods were rotated.

Effects of Electrolyte Concentration. The presence of electrolytes in the aqueous phase has an effect on the electrophoretic mobilities of clays. First, the measured electrophoretic mobility of montmorillonite in the presence of no salt is in quantitative agreement with Swartzen-Allen and Matijevic (*20*). Next, the magnitude of the electrophoretic mobility tends to decrease for an increase in the concentration of electrolyte and corresponding decrease in pH, as shown in Figure 1a. This is in agreement with past research on a variety of clay particles (*20*–*22*).

To investigate the effects of electrolyte concentration on the power requirements and time necessary to clarify the solution, experiments were conducted with varying amounts of sodium chloride in a 0.2 wt % montmorillonite suspension. The effects of increasing salt concentration had the expected result of lowering the instantaneous power requirements during the experiment, as shown in Figure 3a.

It should be pointed out that the electrolyte solutions corresponding to no NaCl addition contained ions originating from the colloidal particles as well as ions formed by dissolution of CO_2 from the ambient air. No attempt was made to eliminate CO_2 or control it. The data shown in Figure 3a for lower ion concentrations show a relative maximum in the instantaneous power consumption at approximately 10 h. This time-dependent power consumption results from the fact that a clear zone forms above the suspension as sedimentation proceeds. The conductivity of the expanding clear zone is less than in the suspension, and as the particle concentration increases, the conductivity increases. The result is that the instantaneous power consumption initially decreases, then goes through a relative maximum, then sharply decreases, and finally slowly increases to a steady-state value.

Figure 3b, which presents information on the solids removal as a function of time, indicates that as the salt level increased, the clarification rate decreased. This is in agreement with the result of a decrease in electrophoretic mobility with a increase in salt concentration. The decrease in mobility is due to the decreased thickness of the electric double layer, as predicted by eq 2, which results in decreasing the repulsive force of the double layer between particles. This leads to an increase in particle–particle interactions and a reduced clarification rate. The increase in the rate of clarification for the experiment with 100 mg/L NaCl compared to the experiment with 50 mg/L NaCl is probably due to the ability

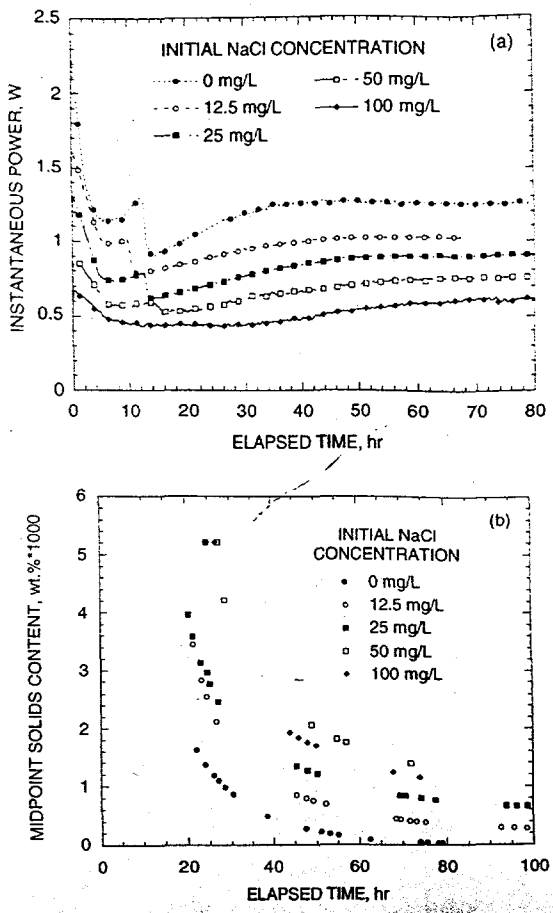

FIGURE 3. Effects of NaCl concentration on (a) the instantaneous power requirements and (b) the rate of solution clarification as measured by the remaining solids content in the clarified solution for batch operation.

of the clay particles to overcome the repulsive forces of the compressed electric double layer, due to electrophoretic motion, leading to particle–particle aggregation and an increased rate of clarification due to gravitational sedimentation.

Effects of Particle Concentration. An increase in the number density of particles in the suspension should cause a decrease in the electrophoretic mobility due to particle–particle hydrodynamic interactions (*16*). This is demonstrated in Figure 1a, which shows an average reduction in electrophoretic mobility of 2.2% for an increase in particle concentration from 0.2 to 0.3 wt %. The magnitude of this reduction in electrophoretic mobility is not predicted by eq 3, which only predicts a reduction of 0.1% for a given ζ potential. Thus, it appears that the reduction in the electrophoretic mobility is due to the increased electrolyte content due to the additional particles. The increase in the electrolyte content is shown by the increase in suspension conductivity with increasing particle concentration in the absence of added salt (Figure 1b).

To investigate the effects of particle concentration on the power requirements and the time necessary to clarify the solution, experiments were conducted with varying amounts of montmorillonite particles in a solution having an NaCl concentration of 12.5 mg/L. Figure 4a shows the increase in time necessary for clarification of the suspension when the initial number density of particles is increased. The corresponding change in instantaneous power required is presented in Figure 4b. The increase in initial conductivity of the suspension with increased solids content lowers the instantaneous power levels for constant current operation.

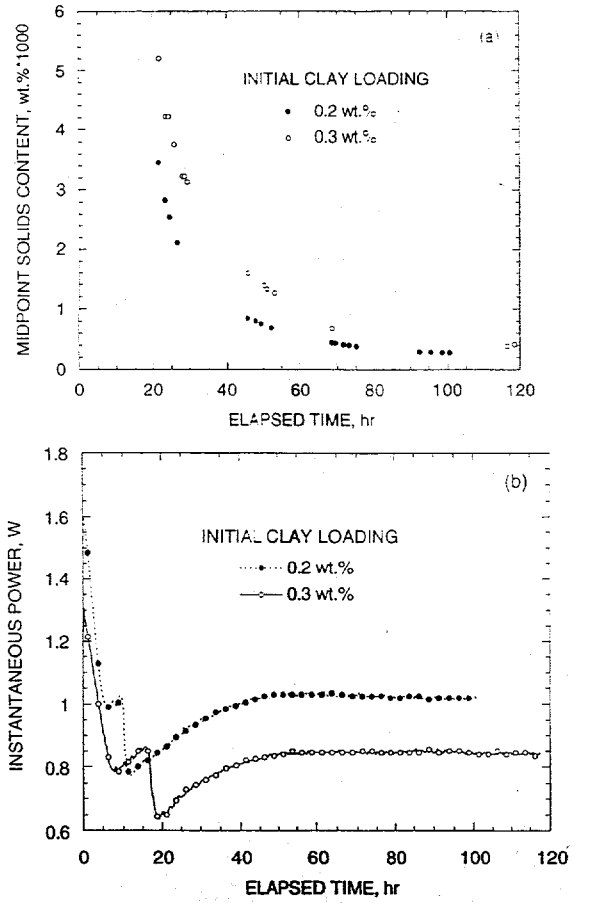

FIGURE 4. Effects of sodium–bentonite concentration on (a) the rate of solution clarification and (b) the instantaneous power requirements for batch operation.

Semicontinuous Experiments. The experiments performed with a batch operation demonstrate the feasibility of clarifying colloidal suspensions electrokinetically, but continuous or semicontinuous operation is preferred for large-scale processing. To demonstrate semicontinuous operation, experiments were performed with a particle concentration of 0.2 wt % and no NaCl added to the RO water.

Initially the experiment was conducted as if it were a batch process. That is, the apparatus was filled with 24 L of the 0.2 wt % colloidal suspension and the electric field was applied. After 48 h the particles had moved below the surface of the anode rods. At this point, more of the 0.2 wt % colloidal suspension was injected beneath the anode rods at a rate of 50 ± 5 mL/min. This method of colloidal addition was thought to be advantageous for two reasons. First, the negative particles would be entering near the anode, and second, the entering particles will have an increased probability of colliding with particles already present in this area. The increased probability of particle collisions increases the chances of particle–particle aggregation which leads to gravitational sedimentation.

Due to the inflow of the added colloidal suspension, the height of the sediment layer rose. Because of this, the addition of the colloidal suspension was periodically stopped every 2 h for a 2 h duration to allow electrophoresis to recompact the sediment. Once the sediment layer dropped to a level near the top of the anode rods, the addition of the colloidal suspension was recommenced. After 13.5 h, 18 L of a 0.2 wt % colloidal suspension had been added to the apparatus and, therefore, 18 L of clarified water with an average solid content of 2.6×10^{-4} wt % had been removed. At this time the sediment layer had increased in height to 8.8 cm above

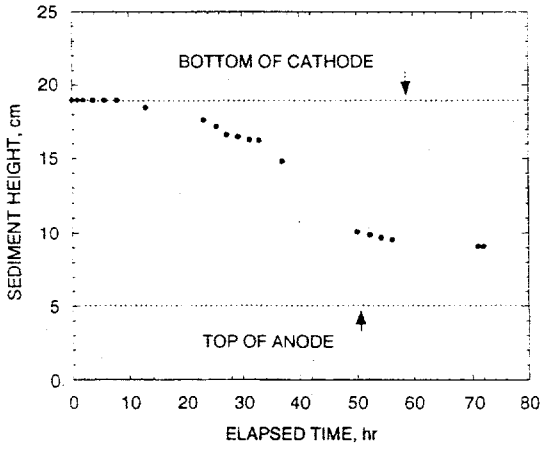

FIGURE 5. Sediment height as a function of time for the processing of the coal-washing wastewater.

the bottom of the tank compared to 2.7 cm at the onset of the semicontinuous operation. By continuing to apply the electric field for an additional 10.5 h, the sediment height reduced to 5.7 cm, resulting in a solid content of 0.757 wt %, an increase of 279% from the original 0.2 wt % suspension. The instantaneous power essentially remained constant at 1.3 W throughout the semicontinuous operation.

It is important to note that eventually the region near the anode will become too concentrated in sedimented particles to achieve effective separation. At this point, the pump can be reversed in order to withdraw the sediment through the inlet tubes.

The benefits in developing a semicontinuous electrokinetic clarification system can be observed from a cost comparison. The operating costs associated with electrokinetic clarification for a system with a flow rate of 25 mL/min, an average power consumption of 1.3 W, and a cost of 12¢/kW·h is approximately 0.010¢/L. Of course, there are additional and unknown costs associated with maintaining the electrokinetic process. Compare this to a typical industrial clarification technique at a coal-washing site which spends about $1.5 M/year on polyelectrolytes to clarify a suspension with an average flow rate of 2270 L/min to give a cost per liter of 0.126¢/L. The primary disadvantage of electrophoretic processing is the rate of clarification, but for cleaning sediment ponds and lakes this is not a serious problem provided the power requirements are low.

Coal-Washing Suspension. To demonstrate that the coal-washing wastewater could be electrophoretically clarified, it was added to the apparatus and clarified in a batch operation. Figure 5 shows the sediment height vs time which resulted in a clarified solution containing 0.018 wt % remaining solids compared to the initial particle concentration of 0.2 wt %. The power level throughout the experiment remained essentially constant at 0.45 W. In this case a sharply defined clear zone did not form, for the suspension remained diffuse as clarification proceeded. As shown in the clay experiments, for higher salt concentrations, the remaining solids content in the clarified solution increases and the power level decreases for higher initial electrolyte concentrations. Therefore, the higher solids content in the clarified solution and the lower power requirement for the coal-washing effluent experiment, compared to the clay experiments, is probably due to the high salt concentration (350 mg/L NaCl) in the wastewater.

Acknowledgments

The authors wish to thank the Department of Energy (Grant DE-FG22-95PC95209) for the financial support of this research and the Oak Ridge Institute for Science and

Education for the funding of summer researchers Gail Furches and Sheryl Filby.

Literature Cited

(1) Grant, C. S.; Matteson, M. J.; Clayfield, E. J. *Sep. Sci. Technol.* **1991**, *26*, 773.
(2) Reuss, F. F. *Mem. Soc. Imp. Nat. Moscow* **1809**. *2*, 3227.
(3) Tiselius, A. *Trans. Faraday Soc.* **1937**, *33*, 524.
(4) Casagrande, L. U.S. Patent No. 2,099,3281, 1937.
(5) Sprute, R. H.; Kelsh, D. J. *Bur. Mines Rep. Invest.* **1982**, No. 8666.
(6) Stanczyk, M. H.; Feld, I. L. *Bur. Mines Rep. Invest.* **1964**, No. 6451.
(7) Lockhart, N. C. *Colloids Surf.* **1983**, *6*, 229.
(8) Wilmans, W.; Van Deventer, J. S. J. *J. S. Afr. Inst. Min. Metall.* **1987**, *87*, 41.
(9) Yoshida, H.; Shinkawa, T.; Yukawa, H. *J. Chem. Eng. Jpn.* **1985**, *18*, 337.
(10) Sauer, J. E.; Davis, E. J. *Environ. Sci. Technol.* **1994**, *28*, 737.
(11) Shang, J. Q.; Lo, K. Y. *J. Hazard Mater.* **1997**, *55*, 117.
(12) Shih, Y. T.; Gidaspow, D.; Wasan, D. T. *Colloids Surf.* **1986**, *21*, 393.
(13) Lee, C.; Gidaspow, D.; Wasan, D. T. Paper presented at the International Powder and Solids Handling and Processing Conference, Philadelphia, PA, 1979.
(14) Matsumoto, K.; Kutowy, O.; Capes, C. E. *Powder Technol.* **1981**, *28*, 205.
(15) Smoluchowski, M. *Handbook of Electricity and Magnetism*, Vol. II; Barth: Leipzig, Germany, 1921; p 366.
(16) Kozak, M. W.; Davis, E. J. *J. Colloid Interface Sci.* **1989**, *127*, 497.
(17) Overbeek, J. Th. G. *Adv. Colloid Sci.* **1950**, *3*, 97.
(18) Wiersema, P. H.; Loeb, A. L.; Overbeek, J. Th. G. *J. Colloid Interface Sci.* **1966**, *22*, 78.
(19) Kozak, M. W.; Davis, E. J. *J. Colloid Interface Sci.* **1989**, *129*, 166.
(20) Swartzen-Allen, S. L.; Matijevic, E. *J. Colloid Interface Sci.* **1976**, *56*, 159.
(21) Sposito, G. *The Surface Chemistry of Soils*; Oxford University Press: New York, 1984.
(22) Chorover, J.; Sposito, G. *Soil Sci. Soc. Am. J.* **1995**, *59*, 1558.

Received for review August 14, 1998. Revised manuscript received January 6, 1999. Accepted January 20, 1999.

ES980835Y

Journal of Colloid and Interface Science 215, 397–408 (1999)
Article ID jcis.1999.6282, available online at http://www.idealibrary.com on IDEAL®

An Analysis of Electrophoresis of Concentrated Suspensions of Colloidal Particles

Timothy J. Johnson and E. James Davis[1]

Department of Chemical Engineering, Box 351750, University of Washington, Seattle, Washington 98195-1750

Received December 14, 1998; accepted April 14, 1999

An analysis of the electrophoretic motion of charged colloidal particles in a concentrated suspension is developed to predict the electrophoretic mobility of the particles and the electrical conductivity of the suspension. The analysis is based on a unit cell model that takes into account particle–particle hydrodynamic interactions and includes relatively thick electric double layers. The fluid motion in the unit cell is treated by writing the relevant Navier–Stokes equation in terms of the stream function and vorticity. The governing equations were then solved by a finite-difference method. The calculated electrophoretic mobilities are in agreement with prior analytical solutions for moderately concentrated suspensions, and the theory reduces to the result of O'Brien and White for low to moderate zeta potentials and dilute suspensions and to the classical result of Smoluchowski for thin double layers and dilute suspensions. A parametric study shows that the electrical conductivity of the suspension relative to a free electrolyte solution is affected by the counterion to co-ion diffusivity ratio, the double-layer thickness, and the volume fraction of particles. For a dispersion of moderately charged particles (moderate zeta potentials) with thick double layers, the numerical model predicts the electrical conductivity in agreement with experimental values reported in the literature.

Key Words: concentrated suspensions; colloidal spheres; electrophoresis; electrical conductivity; fluid mechanics; unit cell model.

INTRODUCTION

The removal of colloidal contaminants from aqueous suspensions can be accomplished by a number of methods, including the addition of alum, acids, bases, and/or polymeric additives to promote agglomeration of the particles so that they will gravitationally sediment. If chemical treatment is undesirable because the clarified water is to be returned to a pond, lake, or water supply, electrophoretic sedimentation offers a possible method of separation. This research was initiated to explore the removal of colloidal coal and clay from lake water and process water contaminated by coal-washing facilities.

Sauer and Davis (1) found that the coal/clay suspension obtained from a lake formerly used to store the effluent from a coal-washing plant near Centralia, Washington, could be clarified electrophoretically using modest potentials and low power consumption. The colloidal contaminants were found to be negatively charged at the nearly neutral pH of the lake water, and the major cation in the surrounding electrolyte solution was sodium.

When an electric field is applied to a suspension of negatively charged particles they will move toward the anode, and the cationic cloud of mobile counterions retards that motion. This phenomenon of electrophoresis was first observed by Reuss (2) nearly 200 years ago, and Smoluchowski (3) developed the first theoretical description of the phenomenon. He analyzed the motion of a single sphere in a fluid of infinite extent with an unpolarized, infinitesimally thin double layer. His well-known expression for electrophoretic mobility, U/E^*, is

$$\frac{U}{E^*} = \frac{\epsilon_r \epsilon_0 \zeta^*}{\mu}, \qquad [1]$$

in which U is the electrophoretic velocity, E^* is the applied electric field, ϵ_r is the dielectric constant of the electrolyte solution, ϵ_0 is the permittivity of free space, ζ^* is the zeta potential, and μ is the fluid viscosity.

The thickness of the double layer, κ^{-1}, where κ is the Debye-Hückel parameter, is given by

$$\kappa = \left(\frac{e^2 \sum_{i=1}^{N} z_i^2 n_i^\infty}{\epsilon_r \epsilon_0 kT} \right)^{1/2}. \qquad [2]$$

Here e is the elementary charge, z_i is the valence of the ith ionic species, n_i^∞ is the number density of the ith ionic species in the electroneutral solution, k is Boltzmann's constant, and T is the absolute temperature. The double layer can be considered thin if $\kappa a^* > 100$, where a^* is the radius of the spherical particle.

Smoluchowski's analysis does not take into account distortion of the double layer due to fluid motion and does not include particle–particle interactions that result in retardation of the motion. Numerous investigators have extended Smoluchowski's theory, relaxing the assumptions made in its development.

Particle–particle interactions become increasingly significant as the number density of particles in a suspension in-

[1] To whom correspondence should be addressed.

0021-9797/99 $30.00

creases. Following on the work of Sauer and Davis, the authors (4) reported representative characteristics of the coal/clay particles from the Centralia coal-washing plant in their study of a laboratory-scale electrophoresis system for water clarification. The water contained moderate concentrations of dissolved salts, and the colloidal particles (1.07 μm volume average diameter) had modest zeta potentials (approx -25 mV). The particles remained suspended because double-layer interactions prevented agglomeration, thereby preventing gravitational sedimentation. The initial solids content of the suspension was typically 0.2 wt%, but as electrophoretic clarification proceeded, the solids content increased substantially in the vicinity of the rotating anodes at the bottom of the tank.

A major concern in electrophoretic clarification of such suspensions is the power requirements, and the prediction of the power consumption requires the ability to determine the electrical conductivity of the suspension. In suspensions of uncharged particles the electrical conductivity of the suspension is nearly that of the surrounding electrolyte solution with a small correction for the presence of the colloidal particles, but for charged particles the electrical conductivity is affected by the thickness and properties of the electric double layer as well as by particle–particle interactions. The objective of this research was to provide such predictive capabilities for the concentrated suspensions involved.

Neale and Nader (5) used a unit cell model to obtain an expression for the ratio of the conductivity of a bed of uncharged spheres, λ_0, to the conductivity of the free solution, λ_∞,

$$\frac{\lambda_0}{\lambda_\infty} = \frac{2(1-\alpha)}{2+\alpha}, \qquad [3]$$

in which α is the volume fraction of colloidal particles. Since the electric double layer has an electrical conductivity different from the bulk electrolyte solution, this geometrical correction is inadequate to describe the conductivity of a suspension of charged colloidal particles. Furthermore, in concentrated suspensions, ionization of surface groups can alter the electrolyte concentration of the bulk solution.

To account for polarizable and thick electric double layers, O'Brien and White (6) numerically solved the complete set of governing equations to determine the electrophoretic mobility of a sphere with an arbitrary zeta potential and double-layer thickness. Ohshima *et al.* (7) later derived a semiempirical relationship valid for relatively thick double layers ($\kappa a^* > 10$), which is in agreement with the results of O'Brien and White. These analyses did not take into account the effects of neighboring particles on the electrophoretic velocity or on the electric field. Ohshima *et al.* did investigate the dependence of charged particles on the electrical conductivity of suspensions, but it cannot be applied to concentrated suspensions since it neglects particle–particle interactions.

Levine and Neale (8) used a unit cell model to account for particle–particle interactions and analyzed the electrophoresis of a swarm of spheres that had low zeta potentials. Later, Kozak and Davis (9) adapted the unit cell model, relaxing the assumption of low zeta potential, and they took into account double-layer distortion (the relaxation effect) to derive an expression for the electrophoretic mobility of a concentrated suspension of spheres. In their first paper they reported the result of thin double layers, $\kappa a^* > 50$, and then they (10) extended the result to apply to moderately thick double layers, $\kappa a^* > 20$. Their analysis reduces to the solution of Ohshima *et al.* for a single sphere in an infinite medium, recovers the Smoluchowski equation in the appropriate limits, and matches the result of Levine and Neale when the zeta potential is sufficiently low. The analyses of Kozak and Davis indicate that the relaxation effect is not significant when the Peclet number is small, that is, when Brownian motion is sufficiently large. The Peclet number is defined by a $*U/D*$, in which D^* is diffusivity of the mobile counterions.

Relatively little theoretical work has been published on the prediction of electrical conductivities in concentrated suspensions, and even less experimental data. The experimental work most often cited is that of Watillon and Stone-Masui (11), who performed conductance studies on a polystyrene latex system of spherical particles and measured the effects of particle charge, zeta potential, and ionic strength of the solution. That work has provided the main source of experimental data with which conductivity theories have been compared.

Dukhin and Derjaguin (12) considered an infinite plane slab of a suspension immersed in an infinite homogeneous electrolyte subjected to an electric field. The conductivity of the suspension was determined by equating the average current in the suspension to the current that would pass through a particle-free electrolyte solution. The electric field within the particle suspension was determined to be a function of the electric dipole strength of the particles. Later, Saville (13) accounted for the relaxation of the electric double layer and used a perturbation method to predict the conductivity of a suspension of particles in the presence of a z–z electrolyte ($z = z_+ = z_-$). The result is a formula that is best determined numerically, and Saville obtained conductivities that underpredicted the experimental data of Watillon and Stone-Masui.

O'Brien (14) solved the governing electrokinetic equations taking into account the relaxation effect, and he derived a formula for the suspension conductivity for a z–z electrolyte. The expression is valid for low zeta potentials and thin double layers and can be evaluated with a hand calculator, but the results also underpredict the experimental results of Watillon and Stone-Masui. Ohshima *et al.* also considered the relaxation effect, and they extended the solution to be valid for higher zeta potentials and thick electric double layers, but their results, too, underpredict the experimental conductivities due to the neglect of particle–particle interactions. The most recent theoretical study that includes particle–particle interactions is that of Kozak and Davis (9). Their result for the conductivity of the

suspension of charged particles, λ_{bed}, relative to the conductivity of the free electrolyte solution, λ_∞, is

$$\frac{\lambda_{bed}}{\lambda_\infty} = \frac{2(1-\alpha)}{2+\alpha} + \left[\frac{6(1-\alpha)\alpha^{1.5}}{(2+\alpha)(1+2\alpha)}\right] \times \left(\frac{1}{1+D_+^*/D_-^*}\right)\left(\frac{K}{1+K}\right), \quad [4]$$

where the parameter K is

$$K = \frac{2(1+2\alpha)}{\kappa a^*(1-\alpha)}\left(1 + \frac{4n_\infty^* kT}{D_-^* \mu \kappa^2}\right)\exp\left(\frac{e|z\zeta^*|}{2kT}\right). \quad [5]$$

Here, D_+^* is the diffusion coefficient of the cations, D_-^* is the diffusion coefficient of the anions, and n_∞^* is the number density of the anions or cations in the electroneutral solution. For a negatively charged particle, D_-^* should replace D_+^*, and vice versa. Equation [4] gives results very close to those of Ohshima *et al.* as $\alpha \to 0$. Therefore, Eq. [4] also underpredicts the experimental results of Watillon and Stone-Masui. This is not surprising since Eq. [4] is valid for particles with thin double layers, whereas the experiments of Watillon and Stone-Masui had thick double layers ($\kappa a^* \approx 1$).

In this paper, a numerical model is developed to solve the governing electrokinetic equations for a suspension of spheres of arbitrary number density with arbitrarily thick, but nonoverlapping, spherical double layers in the presence of a single z–z electrolyte. We do not incorporate the relaxation effect because the particles of particular interest here (coal/clay suspensions) have a low zeta potential and the double layer distortion has been shown to be small for large κa^* ($\kappa a^* \geq 100$ for $|\zeta| \geq 100$ mV) or for small zeta potentials ($|\zeta| \leq 50$ mV when $\kappa a^* \approx 10$) (15, 16). In addition, the Peclet numbers are small, and that substantially reduces retardation due to distortion of the cloud of counterions. Although our computations are restricted to a single z–z electrolyte, the restriction of a z–z electrolyte can be relaxed at the expense of computational time. The result of the numerical model is the determination of the electrophoretic velocity, the electrical conductivity of the suspension, and the effects of electrolyte type and concentration on the measured conductivity.

PROBLEM FORMULATION

Governing Equations for Electrophoretic Velocity and Flow Field

Consider a swarm of spheres undergoing electrophoresis as depicted in Fig. 1. The unit cell model is applied by placing a virtual boundary at radius b^* surrounding each individual particle of radius a^* such that the volume fraction, α, of the unit cell equals the volume fraction of the original suspension. Thus, the volume fraction of particles is given by

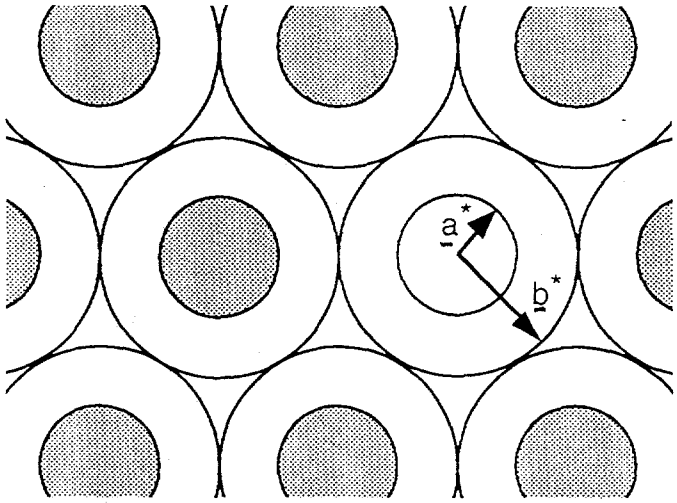

FIG. 1. Spherical unit cell within a concentrated suspension of particles.

$$\alpha = (a^*/b^*)^3. \quad [6]$$

The variables denoted with an asterisk represent dimensional quantities when they appear elsewhere as dimensionless variables.

In this analysis, the unit cell model of Kuwabara (17) was used to solve for the flow field around a particle undergoing electrophoresis. Only the flow around a single particle need be analyzed since Kuwabara's boundary condition of zero vorticity at the outer boundary implicitly accounts for the presence of the surrounding particles. The well-known unit cell model of Happel (18), which assumes zero shear at the virtual surface, has been shown (8) not to reduce to Smoluchowski's result in the limit of $\alpha \to 0$. Furthermore, it has been shown that the flow is irrotational for electrophoresis in an infinite domain (19) and Kuwabara's boundary condition is consistent with that result as $\alpha \to 0$.

The fluid motion within the unit cell is described by the steady-state, creeping-flow form of the Navier–Stokes equation with an additional term that accounts for the electrical body force, $\rho\nabla\Phi_{tot}$, where ρ is the charge density in solution and Φ_{tot} is the total electric potential due to the superposition of the double layer potential, ψ, and the applied electric field, ϕ. The dimensionless Navier–Stokes equation is

$$M\nabla^2\mathbf{u} = \nabla p + \rho\nabla\Phi_{tot}. \quad [7]$$

The parameters and variables have been made dimensionless as follows:

$$M = \frac{\mu U}{a^* n^\infty kT}, \quad \mathbf{u} = \frac{\mathbf{u}^*}{U}, \quad p = \frac{p^*}{n^\infty kT},$$

$$\rho = \frac{\rho^*}{zen^\infty}, \quad \Phi_{tot} = \frac{ze\Phi_{tot}^*}{kT}, \quad r = \frac{r^*}{a^*}.$$

Here p^* is the pressure, and z is the valence of the ions in a z–z electrolyte. The origin is placed at the center of the particle, and the particle is considered to be stationary in the flowing fluid. This is identical to a reference frame in which the particle is moving and the far-field velocity of the fluid is zero.

The solution to Eq. [7] requires knowledge of the potential distribution within the unit cell. The potential associated with the electric double layer is determined by solving Poisson's equation,

$$\nabla^{2*}\psi^* = -\rho^*/\epsilon_r\epsilon_0, \qquad [8]$$

and the charge distribution is related to the ionic number density distribution as follows:

$$\rho^* = \sum_{i=1}^{N} z_i n_i^* e. \qquad [9]$$

For a spherically symmetric electric double layer that is in equilibrium, the ionic number density distribution is determined from the Boltzmann distribution,

$$n_i^* = n_i^\infty \exp\left(-\frac{z_i e \psi^*}{kT}\right). \qquad [10]$$

Combining Eqs. [8]–[10], one obtains the Poisson–Boltzmann equation, which, in dimensionless form for a z–z electrolyte, is

$$\nabla^2\psi = (\kappa a^*)^2 \sinh(\psi). \qquad [11]$$

Here, ψ is a function of the radial component only since the electric double layer is assumed to be spherically symmetric.

The potential due to the applied electric field, ϕ, is governed by Laplace's equation

$$\nabla^2\phi(r, \theta) = 0, \qquad [12]$$

subject to the following boundary conditions at the particle surface and at the outer boundary of the unit cell:

$$\frac{\partial\phi(1, \theta)}{\partial r} = 0, \qquad [13]$$

$$\frac{\partial\phi(b, \theta)}{\partial r} = -\left(\frac{a^*}{L}\right) E \cos(\theta). \qquad [14]$$

The applied electric field, E, is made dimensionless by writing

$$E = \frac{LzeE^*}{kT},$$

where L is the length scale over which the field is applied. Equation [13] applies because no current can pass through the nonconducting particle, while Eq. [14] signifies a uniform electric field strength at the unit cell boundary. The solution of [12] subject to the boundary conditions is

$$\phi(r, \theta) = -\frac{E\cos(\theta)}{(1-\alpha)}\left(\frac{a^*}{L}\right)\left[r + \frac{1}{2r^2}\right]. \qquad [15]$$

To eliminate pressure in the Navier–Stokes equation, we take the curl of Eq. [7] to obtain

$$M\nabla^2\omega = \nabla\rho \times \nabla\Phi_{tot}, \qquad [16]$$

where ω is the fluid vorticity. The fluid flow is assumed to be axisymmetric, and hence the only nonzero component of the vorticity is the azimuthal component, given by

$$\omega_\varphi = \frac{1}{r}\left[\frac{\partial(ru_\theta)}{\partial r} - \frac{\partial u_r}{\partial\theta}\right]. \qquad [17]$$

Since the fluid is incompressible, the equation of continuity becomes

$$\nabla \cdot \mathbf{u} = 0. \qquad [18]$$

This constraint is satisfied by introducing the stream function, ψ_{st}, defined by

$$u_r \equiv -\frac{1}{r^2\sin(\theta)}\frac{\partial\psi_{st}}{\partial\theta}, \qquad [19]$$

$$u_\theta \equiv \frac{1}{r\sin(\theta)}\frac{\partial\psi_{st}}{\partial r}. \qquad [20]$$

Thus, Eqs. [16] and [17] become, respectively,

$$r^2\frac{\partial^2 g}{\partial r^2} + \frac{\partial^2 g}{\partial\theta^2} - \cot(\theta)\frac{\partial g}{\partial\theta} = \frac{r^2\sin(\theta)}{M}\frac{\partial\rho}{\partial r}\frac{\partial\phi}{\partial\theta}, \qquad [21]$$

and

$$r^2\frac{\partial^2\psi_{st}}{\partial r^2} + \frac{\partial^2\psi_{st}}{\partial\theta^2} - \cot(\theta)\frac{\partial\psi_{st}}{\partial\theta} = r^2 g, \qquad [22]$$

where g is defined as $g = \omega_\varphi r\sin(\theta)$. Inserting Eq. [10] into

Eq. [9]. making the result dimensionless, inserting the result in Eq. [21], and using Eq. [15], one obtains

$$r^2\frac{\partial^2 g}{\partial r^2}+\frac{\partial^2 g}{\partial \theta^2}-\cot(\theta)\frac{\partial g}{\partial \theta} = -\frac{2E\sin^2(\theta)\cosh(\psi)}{M(1-\alpha)}\frac{\partial \psi}{\partial r}\left[r^3+\frac{1}{2}\right]\left(\frac{a^*}{L}\right). \quad [23]$$

Equations [11], [22], and [23] are the governing equations that must be solved to obtain the desired properties of the system. Equation [11] is solved subject to the boundary conditions

$$\psi(1,\theta)=\zeta, \quad [24]$$

$$\left.\frac{\partial \psi}{\partial r}\right|_{r=b,\theta}=0. \quad [25]$$

Equation [24] is an approximation that is valid if the shear layer at which the zeta potential is defined is placed very close to the surface of the particle. The boundary conditions associated with Eqs. [22] and [23], the stream function-vorticity equations, are

$$g(r,0)=g(r,\pi)=\psi_{st}(r,0)=\psi_{st}(r,\pi)=0, \quad [26]$$

$$g(1,\theta)=\left.\frac{\partial^2 \psi_{st}}{\partial r^2}\right|_{r=1,\theta}, \quad [27]$$

$$g(b,\theta)=0, \quad [28]$$

$$\psi_{st}(1,\theta)=\left.\frac{\partial \psi_{st}}{\partial r}\right|_{r=1,\theta}=0, \quad [29]$$

$$\psi_{st}(b,\theta)=\frac{1}{2}b^2\sin^2(\theta). \quad [30]$$

Equation [28], which represents zero vorticity at the virtual surface, is the Kuwabara boundary condition discussed above.

The Electrical Conductivity of a Suspension

The electrical conductivity of a suspension of charged spheres in an electrolyte solution can be determined once the flow field within the system is known. To determine the electrical conductivity, both the conductivity of the electric double layer and the geometric effects due to the presence of the nonconducting particles must be taken into account. Following Kozak and Davis (9), the contribution of the electric double layer to the suspension conductivity begins with determining the total current that enters into the upper half of the unit cell. The total current over this surface is

$$I_{r=b}=2\pi b^2\int_0^{\pi/2} i_z\sin\theta\cos\theta d\theta, \quad [31]$$

where

$$i_z=i_\theta\sin\theta-i_r\cos\theta, \quad [32]$$

and

$$i_\theta(r,\theta)=u_\theta(r,\theta)(n_- - n_-)-\frac{1}{r}\frac{\partial \phi}{\partial \theta}(D_- n_+ + D_- n_-), \quad [33]$$

$$i_r(r,\theta)=u_r(r,\theta)(n_- - n_-)-\frac{\partial \phi}{\partial r}(D_+ n_- + D_- n_-). \quad [34]$$

Here, i_θ and i_r are the angular and radial component of the current density, respectively, for a spherically symmetric double layer. Equation [31] represents the current that would pass through a particle-free solution since it is evaluated at the outer boundary. The ion diffusion is neglected in Eq. [31] since gradients in the ion number density will be zero at the outer boundary according to Eq. [25].

Next, to account for the effect of the electric double layer on the total current, it is convenient to determine the current within the unit cell at the plane $\theta=\pi/2$ because the radial contribution of the current flux vanishes. Thus, the total current at this plane, in dimensionless form, can be expressed as

$$I_{\pi/2}=2\pi\int_1^b i_\theta(r,\pi/2)rdr. \quad [35]$$

Equations [31] and [35] were integrated using the trapezoidal rule.

The conductivity of the particle swarm, λ_{bed}, relative to the conductivity of the particle swarm in the absence of double layer effects, λ_0, is the ratio of Eq. [35] and Eq. [31], that is,

$$\frac{\lambda_{bed}}{\lambda_0}=\frac{2\pi\int_1^b i_\theta(r,\pi/2)rdr}{2\pi b^2\int_0^{\pi/2} i_z\sin\theta\cos\theta d\theta}. \quad [36]$$

The last step is to account for the effect of the presence of the particles on the conductivity of the solution using the unit cell result of Neale and Nader (5), Eq. [3]. Combining Eqs. [36] and [3] gives the ratio of the conductivity of a bed of charged spheres in an electrolyte solution, λ_{bed}, to the conductivity of a pure electrolyte solution, λ_∞:

$$\frac{\lambda_{bed}}{\lambda_\infty}=\left[\frac{2(1-\alpha)}{2+\alpha}\right]\frac{2\pi\int_1^b i_\theta(r,\pi/2)rdr}{2\pi b^2\int_0^{\pi/2} i_z\sin\theta\cos\theta d\theta}. \quad [37]$$

NUMERICAL METHOD

The set of governing equations, Eqs. [11], [22], and [23], subject to the associated boundary conditions, was solved numerically. The difficulty in solving the Navier–Stokes equa-

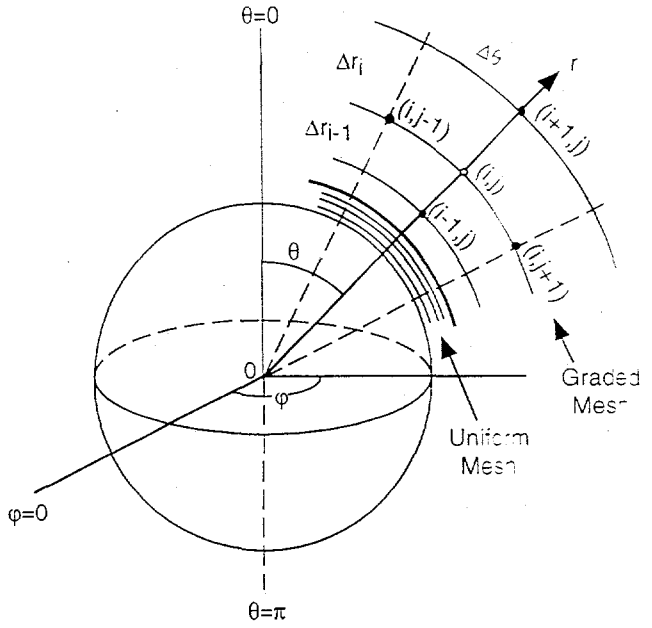

FIG. 2. Spherical polar coordinate system and schematic of the generated mesh.

tion for flow around a charged particle is due to the presence of the relatively thin electrical double layer within the domain of the unit cell. Within this region the vorticity, the ionic concentration, and the potential decay from their interfacial values to the bulk solution values within a very short distance from the surface of the sphere. A fine uniform grid was used in this thin region, and a graded mesh was employed throughout the rest of the domain. A schematic of the mesh generated is shown in Fig. 2. Due to axisymmetric flow, the computational domain was decreased further by carrying out calculations only for the region between $\theta = 0$ and π.

To numerically approximate the differential equations, the standard second-order finite-difference equations for a uniform mesh were used in the fine region. In the graded region, the following nonuniform-centered finite-difference equations were used. They are derived from a Taylor series expansion and reduce to the standard second-order equations for a uniform mesh:

$$\left.\frac{\partial \Gamma}{\partial r}\right|_i = \frac{\Gamma_{i+1} + (\nu^2 - 1)\Gamma_i - \nu^2 \cdot \Gamma_{i-1}}{\Delta r_i(\nu + 1)}, \quad [38]$$

$$\left.\frac{\partial^2 \Gamma}{\partial r^2}\right|_i = \frac{\Gamma_{i+1} - (\nu + 1)\Gamma_i + \nu \cdot \Gamma_{i-1}}{\frac{1}{2}\Delta r_{i-1}\Delta r_i(\nu + 1)}. \quad [39]$$

where $\nu = \Delta r_i/\Delta r_{i-1}$. Here Γ represents either the potential, ψ, the stream function, ψ_{st}, or the vorticity, g, and Δr represents the radial step in the r-direction. Since the nonuniform finite-difference equations decrease from second-order accuracy as ν deviates from unity, ν was kept below 1.25.

Equation [25] at the outer boundary was approximated by the following one-sided, nonuniform, finite-difference equation:

$$\left.\frac{\partial \psi}{\partial r}\right|_{r=b,j} = \frac{1 + 2\nu}{\Delta r_b(1 + \nu)}\psi_{b,j} - \frac{1 + 2\nu + \nu^2}{\Delta r_b(1 + \nu)}\psi_{b-1,j} + \frac{\nu}{\Delta r_{b-1}(1 + \nu)}\psi_{b-2,j} = 0, \quad [40]$$

where $\nu = \Delta r_b/\Delta r_{b-1}$. Equation [27] was approximated at the surface by a second-order Lagrange polynomial. Inserting Eq. [29] into the finite-difference form of Eq. [27] for a uniform radial mesh gives

$$g(1, \theta) = \left.\frac{\partial^2 \psi_{st}}{\partial r^2}\right|_{r=1,j} = \frac{\psi_{st;a+2,j} - 2\psi_{st;a+1,j}}{\Delta r^2}. \quad [41]$$

The variables in Eqs. [40] and [41] are pictorially represented in Fig. 3.

The solution to the set of nonlinear algebraic equations resulting from the finite-difference form of the Poisson–Boltzmann equation for a z–z electrolyte was obtained by using a Gauss–Newton method with a mixed quadratic and cubic line search procedure. This method is a standard subroutine (referred to as fsolve) within the professional version of MathWorks, Inc., Matlab computational software. The default convergence criterion of 1×10^{-4} was used for the calculations.

Once the solution to the charge distribution was obtained, the solution to the stream function-vorticity equations commenced. The final solution to the set of equations was reached by an iterative procedure. First, the set of linear algebraic equations obtained by the finite-difference representation of the vorticity equation, Eq. [23], subject to boundary conditions [26], [27], and [28], was solved using the Crout decomposition (20). Second, one iteration was performed on the set of linear algebraic equations for the stream function equation, Eq. [22], with boundary conditions [26], [29], and [30]. The equations were solved by incorporating a time derivative in Eq. [22], and then using the alternating direction implicit (ADI) method (20). The time step, Δt, in the time derivative acts as an adjustable relaxation parameter to control the stability of the solution and is equivalent to the relaxation parameter β given by Peaceman

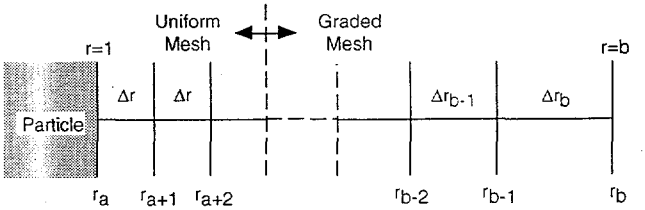

FIG. 3. Schematic of the mesh system with significant variables labeled which are used in Eqs. [40] and [41].

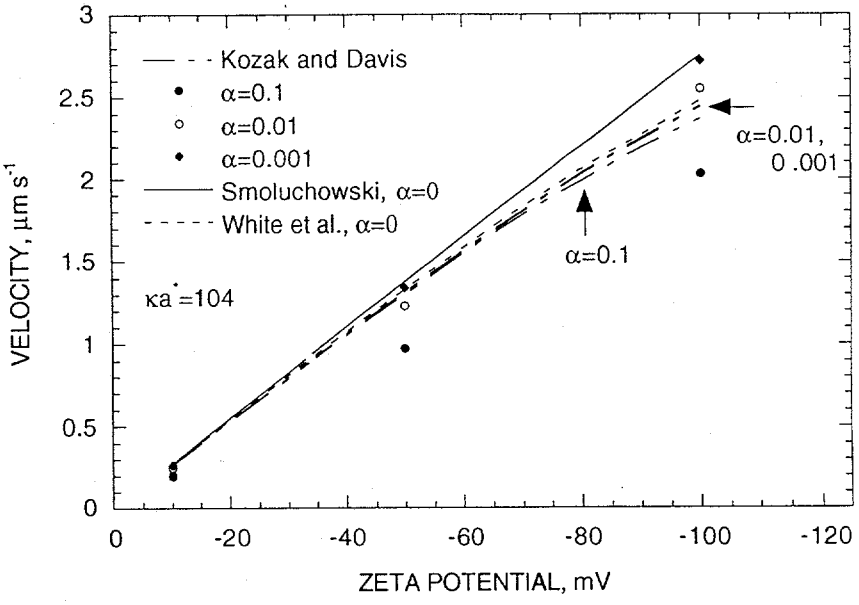

FIG. 4. The electrophoretic velocity for various volume fractions of particles with thin double layers as computed by Kozak and Davis (10), our numerical model, Smoluchowski's equation (Eq. [1]), and White *et al.* (22).

(21) by the formula $2/\Delta t = \beta$. While Peaceman discusses accelerated convergence rates by using cyclic relaxation parameters, this failed to work for the current problem, and the maximum time step that maintained stability was $\Delta t = 4 \times 10^{-6}$. After completion of a single iteration on Eq. [22], the vorticity equation, Eq. [23], was solved again and the procedure was repeated until the stream function and vorticity values reached the convergence criteria. The convergence criteria for the stream function and vorticity values were 1×10^{-6} and 5×10^{-5}, respectively.

The complexity of solving the governing equations for the electrophoresis of a swarm of particles stems from the fact that the far-field velocity, U, is not known *a priori,* because it depends on the particle charge and the strength of the applied electric field. To obtain the correct solution, the governing equations were solved for a trial far-field velocity. If the chosen velocity is correct, the theta component of the velocity at $\pi/2$ and at the outer boundary is unity, $u_\theta(b, \pi/2) = 1$, since the Navier–Stokes equation was made dimensionless by the far-field velocity. It should be noted that the stream function-vorticity equations along with their boundary conditions do not automatically satisfy the criterion of $u_\theta(b, \pi/2) = 1$. Once a solution to the stream function-vorticity equations is obtained, the value of $u_\theta(b, \pi/2)$ can be determined by using the finite-difference formula of Eq. [40] in Eq. [20]. If the initial estimate for the far-field velocity is too high, the calculated $u_\theta(b, \pi/2) > 1$, and if the trial value is too low, $u_\theta(b, \pi/2) < 1$. The convergence criterion for the chosen far-field velocity was such that the calculated value of $u_\theta(b, \pi/2)$ must fall in the range of 1.0 ± 0.005 after the convergence criterion is satisfied.

RESULTS

Electrophoretic Velocity

To investigate the effects of particle concentration, double-layer thickness, and zeta potential on the electrophoresis of a swarm of particles, solutions of the numerical model were obtained for volume fractions corresponding to the range 0.1–10% solids, for double-layer thicknesses in the range $\kappa a^* = 7.35$–104, and for zeta potentials ranging from -10 to -100 mV. The other parameters held constant were $E^* = -35.7$ V m^{-1}, $\epsilon_r = 78.5$, $T = 298$ K, and $\mu = 9.01 \times 10^{-4}$ kg m^{-1} s^{-1}. These correspond to the experimental conditions reported by Johnson and Davis (4).

The electrophoretic velocity obtained from the numerical model should approach Smoluchowski's solution, Eq. [1], as $\alpha \to 0$ and for $\kappa a^* \gg 1$. This is confirmed for a suspension of particles with $\kappa a^* = 104$, as shown in Fig. 4. Also plotted is the analytical result of Kozak and Davis (10) and the numerical result of MacMobility, a program developed by White *et al.* (22) based on the work of O'Brien and White (6). The results of White *et al.* and Kozak and Davis include the relaxation effect, and the latter was developed for moderately thick double layers ($\kappa a^* > 20$). For the calculations using MacMobility and in the analytical result of Kozak and Davis, KCl was chosen as the electrolyte. Figures 5 and 6 display additional information for $\kappa a^* = 50$ and 7.35, respectively. The results show the expected behavior of a reduction in the electrophoretic velocity as particle–particle interactions and double-layer interactions between the particles cause a resistance to movement.

Comparison of our results with the numerical results of

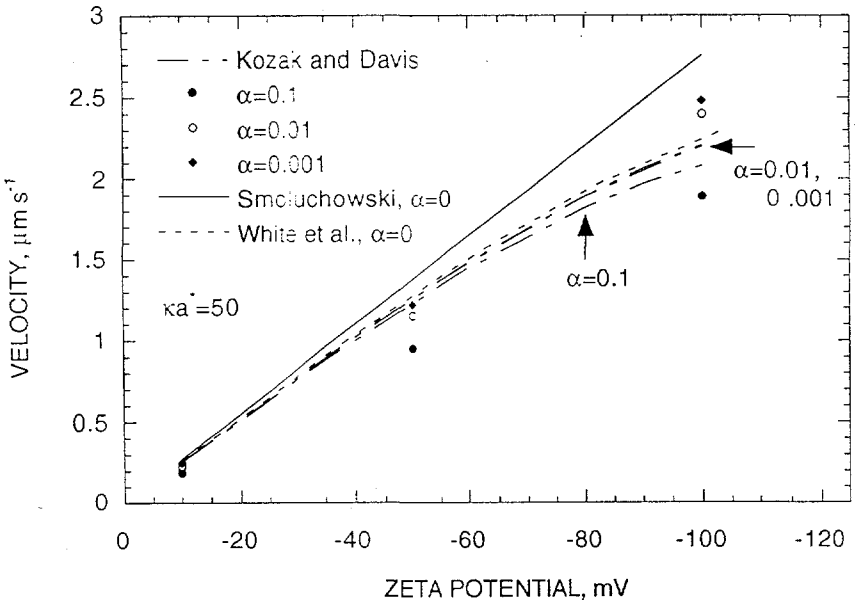

FIG. 5. The electrophoretic velocity for various volume fractions of particles with moderately thick electric double layers.

MacMobility show that the neglect of the relaxation effect is valid for particles with $|\zeta| \leq 50$ mV. The differences in the electrophoretic velocity for $|\zeta| \leq 50$ mV, as determined by our model and Kozak and Davis, are a result of the very different methods applied to obtain a solution. Kozak and Davis linearized the governing equations and made approximations to integrals involved in the analysis to obtain an analytical solution, whereas our model was limited only by the accuracy of the finite-difference method. The next section will show that the approximations made to obtain an analytical solution lead to an underprediction for the relative conductivity of a colloidal dispersion.

Relative Conductivity

The relative conductivity of the suspensions considered in the previous section were determined from the flow field that transported the ions. Figure 7 displays the relative conductivity of a suspension of negatively charged particles in various electrolytes with cation/anion diffusivity ratios of 4.6:1, 0.5:1,

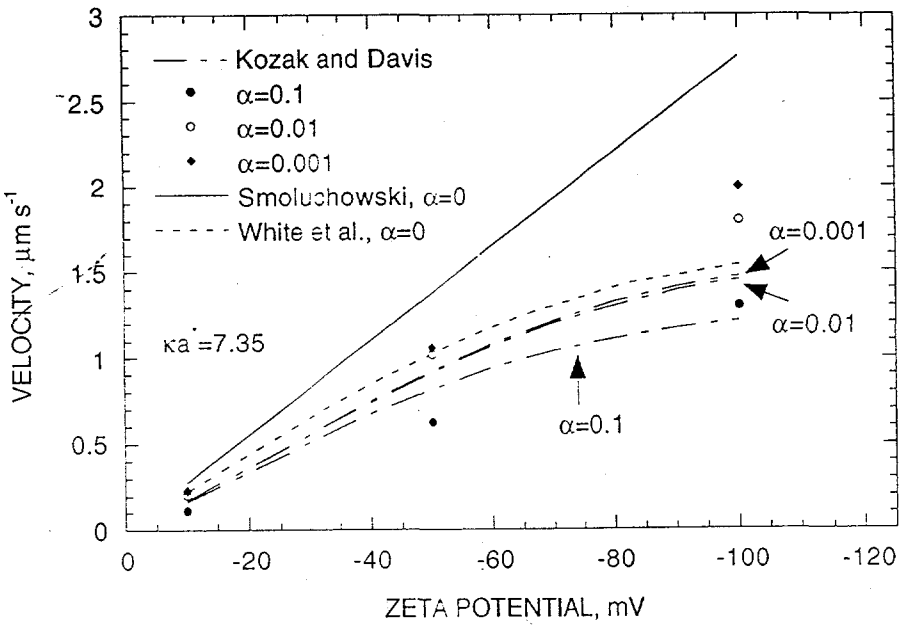

FIG. 6. The electrophoretic velocity for various volume fractions of particles with thick electric double layers.

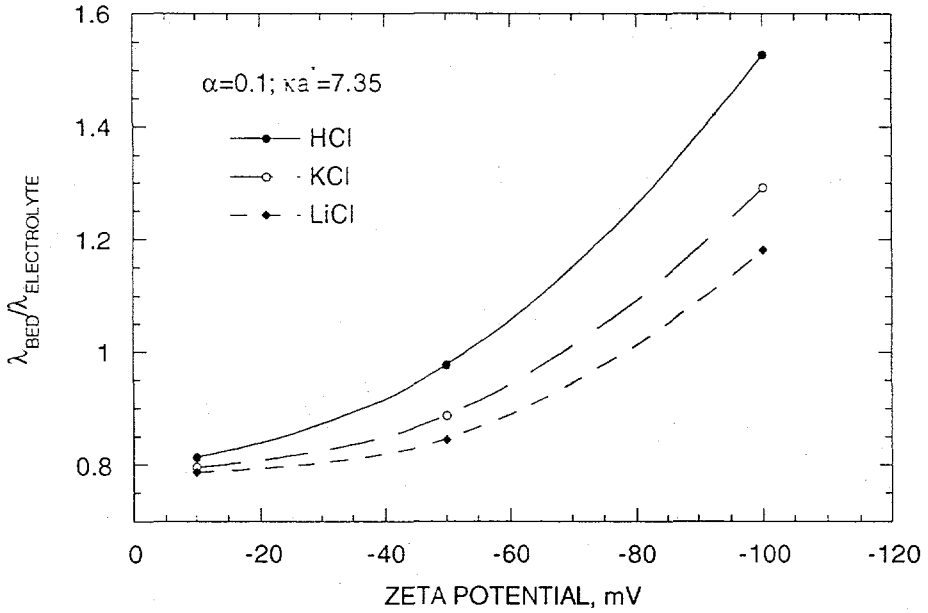

FIG. 7. Numerical results for the relative conductivity of a concentrated suspension of spheres as a function of zeta potential and electrolyte type.

and 1:1 for HCl, LiCl, and KCl, respectively. The results show that the increase in relative conductivity due to the presence of the double layer, for a given zeta potential, decreases as the counterion to co-ion diffusivity ratio decreases. Also, for a given zeta potential and an electrolyte with a diffusivity ratio less than 1:1 the relative conductivity can either increase or decrease as κa^* decreases, as shown in Fig. 8. The decrease in relative conductivity as κa^* decreases is due to the large contribution of mobile co-ions, as discussed by Watillon and Stone-Masui (11).

The relative conductivity is also dependent on the volume fraction of particles in suspension. There are two competing effects: (1) the presence of the nonconducting particles tends to lower the relative conductivity, and (2) the surface conductance within the double layer acts to increase or decrease the relative conductivity depending on the zeta potential and the supporting electrolyte type and concentration. For high zeta potentials and thick double layers, Fig. 9 shows the changes in the relative conductivity for an increase in the volume fraction of particles. As the volume fraction of particles is decreased,

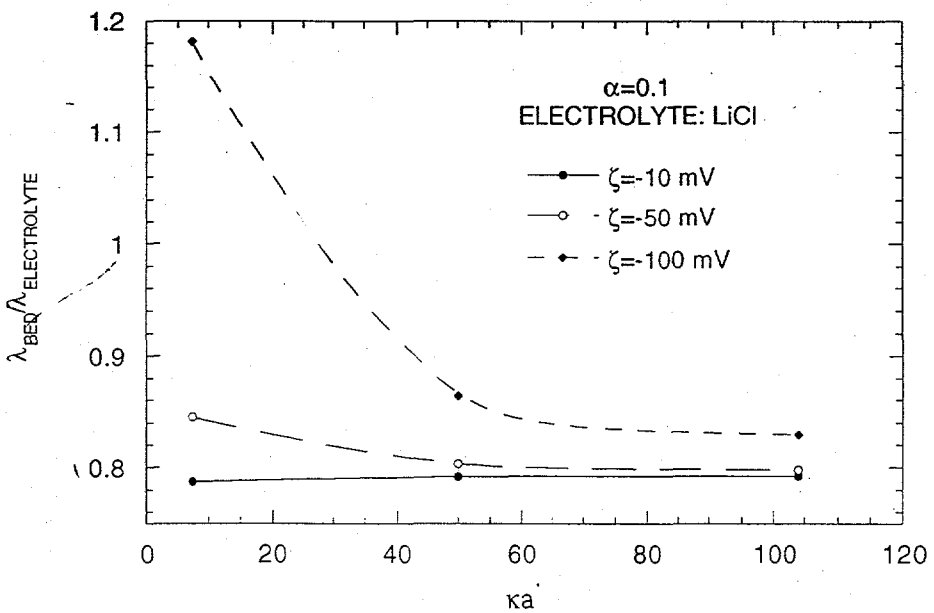

FIG. 8. Results for the relative conductivity of a concentrated suspension of spheres in a LiCl electrolyte, as a function of κa^* and zeta potential. Note the decrease in relative conductivity, as κa^* decreases, for a swarm of particles with a zeta potential of -10 mV.

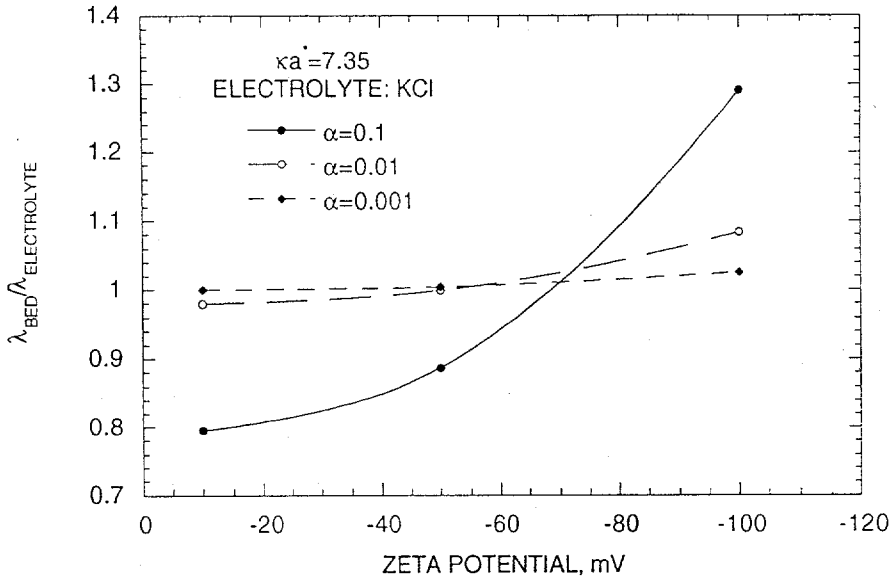

FIG. 9. Numerical results for the relative conductivity of a suspension of spheres in a KCl electrolyte, as a function of zeta potential and volume fraction.

the effects of surface conductance become negligible, and the relative conductivity remains near unity.

Next, the numerical model was used to predict the electrical conductivities of the systems investigated by Watillon and Stone-Masui (11). They prepared and measured the conductivity of a suspension of polystyrene latex spheres in various electrolytes for several zeta potentials. Unfortunately, only two of the experiments could be compared with our model because the other experiments used more than one electrolyte or, as Saville (13) discussed, the actual ionic strength is unknown. The two experiments of Watillon and Stone-Masui compared with our model were (1) a suspension of 70-nm-diameter spheres having a zeta potential of -62.2 mV in 0.1 mM $HClO_4$ (suspension 1 of Watillon and Stone-Masui) and (2) a suspension of 56-nm-diameter spheres with a zeta potential of -99 mV in 0.1 mM $HClO_4$ (suspension 11 of Watillon and Stone-Masui).

The experimental data for the relative conductivity of suspensions 1 and 11 were compared with results from our numerical model, from Eq. [4], and from O'Brien (14). For the experimental data, the conductivity of the electrolyte was taken to be the extrapolated value at zero volume fraction (Fig. 4 of Watillon and Stone-Masui). The addition of a large number density of particles to an electrolyte solution can alter the ion concentration of the bulk solution due to dissociation of surface groups. In addition, dissolved CO_2 can increase the concentration of ions. Watillon and Stone-Masui purified their aqueous dispersions prior to electrolyte addition by using a mixed-bed ion-exchange resin to remove cations present due to the dissociation of surface groups. Furthermore, the colloidal solutions were prepared avoiding atmospheric CO_2 by using a nitrogen blanket. Thus, the extrapolation to zero volume fraction seems reasonable.

It should be noted that suspensions 1 and 11 have κa^* values of 1.15 and 0.92, which is well below the limit of applicability for the analysis of Kozak and Davis (9). Also, the analysis of O'Brien neglects the effects of surrounding particles. Since the κa^* values are low, even dilute suspensions will have particle–particle interactions due to the extended double layer. For suspension 1 the onset of double-layer overlap occurs around a volume fraction of 0.0101, while double-layer overlap occurs around a volume fraction of 0.0063 for suspension 11.

Figure 10 compares the predictions of the relative conductivities for suspension 1. It can be seen that Kozak and Davis and O'Brien underpredict the experimental results by as much as 14% at a volume fraction of 0.0101, whereas the numerical model slightly overpredicts the relative conductivity by 2.4%. The success of the numerical model marks the first time that a theoretical analysis for the relative conductivity of a suspension of charged spheres has been reasonably matched to experimental data. It is felt that the overprediction of the relative conductivity compared to the experimental data is due to the neglect of the relaxation effect.

The neglect of the relaxation effect in our prediction for the relative conductivity is more evident for suspension 11 in which the particles have a more negative zeta potential. Figure 11 compares the predictions of the relative conductivities for suspension 11. It is shown that the theory of Kozak and Davis underpredicts the experimental data by 24% at a volume fraction of 0.0063, the theory of O'Brien underpredicts the data by 18%, and our numerical model overpredicts the data by 26%.

SUMMARY

We have developed a numerical method, using Kuwabara's unit cell model and the stream function-vorticity formulation of the Navier–Stokes equation, to model a concentrated suspen-

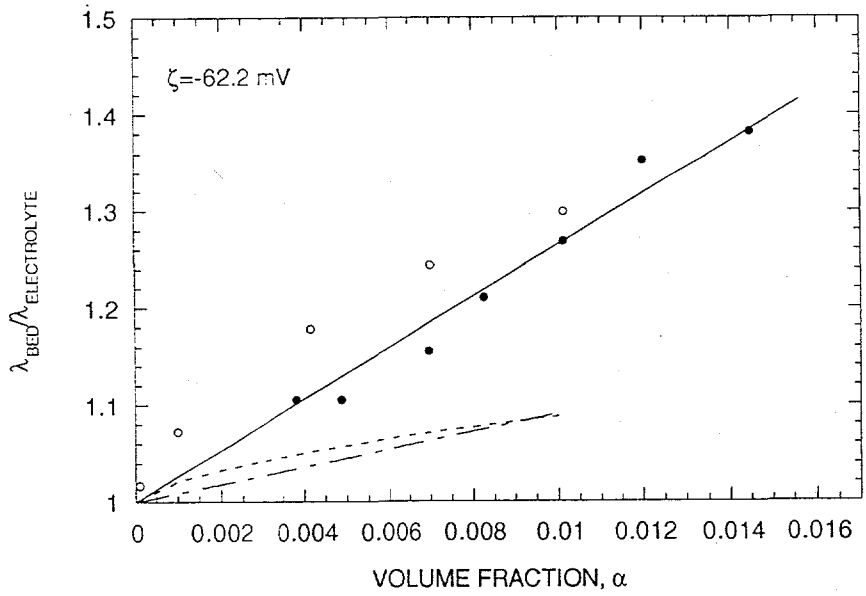

FIG. 10. Comparison of the relative conductivity of a suspension of 70-nm-diameter spheres with a zeta potential of −62.2 mV in the presence of 0.1 mM $HClO_4$ as determined by: Watillon and Stone-Masui (11) (●), our numerical model (○), Kozak and Davis (9) (– – –), and O'Brien (14) (— · —).

sion of spheres with symmetric double layers that undergo electrophoresis. The predicted electrophoretic velocities correctly reduce to Smoluchowski's solution in the limit of low volume fractions and thin double layers, and the model gives results similar to those of Kozak and Davis (10) for moderately thick double layers in concentrated suspensions.

A parametric study was also performed to explore the effects of electrolyte type and concentration on the relative conductivity of a suspension of charged particles within an electrolyte. It was shown that increases in the counterion to co-ion diffusivity ratio tend to increase the relative conductivity for a given zeta potential and double layer thickness. For electrolytes with counterion to co-ion diffusivity ratios less than 1:1, it is also possible to cause the relative conductivity to decrease as the double-layer thickness increases. In addition, it was shown that increases in the particle volume fraction lead to marked changes in the relative conductivity of suspensions.

Finally, for a suspension of moderately charged particles ($\zeta^* = -62$ mV) with thick double layers ($\kappa a^* = 1.15$), we have demonstrated that this unit cell model yields better agreement

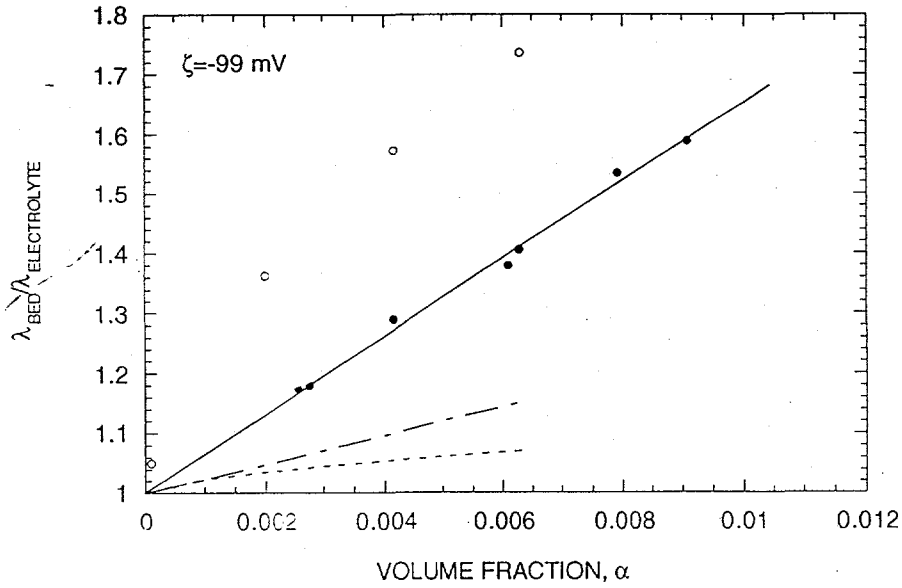

FIG. 11. Comparison of the relative conductivity of a suspension of 56-nm-diameter spheres with a zeta potential of −99 mV in the presence of 0.1 mM $HClO_4$. Legend is the same as in Fig. 10.

with the relative conductivities measured by Watillon and Stone-Masui than previous analyses. As the zeta potential becomes more negative, the relative errors between the numerical model and the experimental data increase, probably due to the neglect of the relaxation effect.

ACKNOWLEDGMENTS

The authors thank the Department of Energy University Coal Research Program (DE-FG22-95PC95209) for its financial support of this research.

REFERENCES

1. Sauer, J. E., and Davis, E. J., *Environ. Sci. Technol.* **28,** 737 (1994).
2. Reuss, F. F., *Mem. Soc. Imp. Naturalistes Moscou* **2,** 327 (1809).
3. Smoluchowski, M., *Z. Phys. Chem.* **92,** 129 (1918).
4. Johnson, T. J., and Davis, E. J., *Environ. Sci. Technol.* **33,** 1250 (1999).
5. Neale, G. H., and Nader, W. K., *AIChE J.* **19,** 112 (1974).
6. O'Brien, R. W., and White, L. R., *J. Chem. Soc. Faraday Trans.* **74,** 1607 (1978).
7. Ohshima, H., Healy, T. W., and White, L. R., *J. Chem. Soc. F2* **79,** 1613 (1983).
8. Levine, S., and Neale, G. H., *J. Colloid Interface Sci.* **47,** 520 (1974).
9. Kozak, M. W., and Davis, E. J., *J. Colloid Interface Sci.* **127,** 497 (1989a).
10. Kozak, M. W., and Davis, E. J., *J. Colloid Interface Sci.* **129,** 166 (1989b).
11. Watillon, A., and Stone-Masui, J., *J. Electroanal. Chem.* **37,** 143 (1972).
12. Dukhin, S. S., and Derjaguin, B. V., "Surface and Colloid Science." Wiley, New York, 1974.
13. Saville, D. A., *J. Colloid Interface Sci.* **71,** 477 (1979).
14. O'Brien, R. W., *J. Colloid Interface Sci.* **81,** 234 (1981).
15. Overbeek, J. T. G., "Advances in Colloid Science," Vol. 3. Interscience, New York, 1950.
16. Wiersema, P. H., Loeb, A. L., and Overbeek, J. Th. G., *J. Colloid Interface Sci.* **22,** 78 (1966).
17. Kuwabara, S., *J. Phys. Soc. Jpn.* **14,** 527 (1959).
18. Happel, J., *AIChE J.* **4,** 197 (1958).
19. Morrison, F. A., *J. Colloid Interface Sci.* **34,** 210 (1970).
20. Chapra, S. C., and Canale, R. P., "Numerical Methods for Engineers," 2nd ed. McGraw–Hill, New York, 1988.
21. Peaceman, D. W., "Fundamentals of Numerical Resevoir Simulations." Elsevier, Amsterdam, 1977.
22. White, L. R., Mangelsdorf, C., and Chan, D. Y. C., Computer Code "MacMobility," University of Melbourne, Parkville, Australia, 1989.

Appendix C. Submitted Paper to *Environmental Science and Technology* (8/11/99)

Experimental Data and Theoretical Predictions for the Rate of Electrophoretic Clarification of Colloidal Suspensions

Timothy J. Johnson and E. James Davis*

Department of Chemical Engineering, Box 351750

University of Washington

Seattle, WA 98195-1750

* Author to whom correspondence should be addressed

Abstract

An experimental and theoretical investigation of the electrophoretic clarification rate of colloidal suspensions was conducted. The suspensions included a coal-washing effluent and a model system of TiO_2 particles. A parametric study of TiO_2 suspensions was performed to validate an analysis of the electrophoretic motion of the clarification front formed between a clear zone and the suspension. To measure the electric field strength needed in the prediction of the location of the front, a moveable probe and salt bridge were connected to a reference electrode. Using the measured electric field strengths, it was found that the numerical solution to the unit cell electrophoresis model agrees with the measured clarification rates. For suspensions with thick electric double layers and high particle volume fractions (α= 0.3% or 1.2 wt%) the deviations from classical Smoluchowski theory are substantial, and the numerical analysis is in somewhat better agreement with the data than a prior solution of the problem. The numerical model reduces to the predictions of previous theories as the thickness of the electric double layer decreases, and it is in good agreement with the clarification rate measured for a coal-washing effluent suspension (α= 0.411% or 0.493 wt%) with thin electric double layers (κa = 144).

Keywords: electrophoresis, colloids, electric field, concentrated suspensions, unit cell model

Introduction

An environmental problem associated with the preparation of coal for coal-fired power plants is the production of a polydisperse, colloidally contaminated aqueous suspension of coal and clay produced from the coal washing process. Due to the surface charge and the small size of the particles, a stable colloidal suspension is formed which does not undergo gravitational sedimentation at acceptable rates. The consolidation technique that is most often used for treating the effluent from coal washing and other contaminated streams is the addition of high molecular weight polyelectrolytes or other chemical additives. For example, Grant *et al.* (1) used a surfactant (sodium dodecyl sulfate or cetyltrimethylammonium bromide) and found that the rate and extent of dewatering of iron oxide fines increased with increasing surfactant concentration. Clarification via surfactant or polyelectrolyte addition can be expensive, and there is concern about discharging the treated fluid to the environment after it has been chemically altered.

An alternative clarification technique, which has been known for several decades and is chemically non-invasive, and possibly less costly, is the application of an electric field to the colloidal suspension to achieve separation electrokinetically. When an electric field is applied to the suspension, the particles will move in the direction of the electric field lines. This phenomena of particle movement relative to the surrounding stagnant fluid, due to an applied electric field, is known as *electrophoresis*, and it results from the fact that the colloidal particles become charged in water at the typical pH's encountered. In 1809 Reuss (2) observed this phenomena and the related phenomenon of *electroosmosis* in which the fluid moves through a stationary porous medium due to the applied electric field.

In the 1930's the electrokinetic phenomena was applied to various processes, including the separation of proteins (3) and the stabilization of soft soils (4). In the 1960's Sprute and Kelsh (5) at the Bureau of Mines carried out a number of investigations on the use of electrokinetics for the densification of mill tailings and coal-processing waste. Stanczyk and Feld (6), also at the Bureau of Mines, investigated electrokinetics for dewatering phosphate clays.

Since the Bureau of Mines investigations, several other researchers have explored the use of electrokinetics as a separation technique. Lockhart (7) was able to clarify clay suspensions and mine tailings, Wilmans and Van Deventer (8) treated kimberlite slimes from diamond mining, and Yoshida *et al.* (9) treated bentonite sludge. Sauer and Davis (10) and Johnson and Davis (11) were able to consolidate a coal-washing effluent suspension. Electrophoresis has also been applied to colloidal suspensions in non-aqueous media. Shih *et al.* (12) investigated the sedimentation of illite particles in toluene containing asphaltene, Lee *et al.* (13) studied the rate of sedimentation of α-alumina particles in xylene for various concentrations of a surfactant which controlled the surface charge on the particles, and Matsumoto *et al.* (14) removed oxidized aluminum and iron particles from kerosene.

Successful laboratory studies have not yet led to widespread commercial application. This can be partly attributed to the low rates of particle migration in an electric field and partly to a poor understanding of particle motion in concentrated suspensions when an electric field is applied. The latter issue makes it difficult to scale up results from the laboratory to commercial sizes.

Numerous analyses of single particle motion in an electric field have been published. The first analysis of electrophoretic motion was that of Smoluchowski (15)

for a single sphere with a low surface potential and a nonpolarizable thin electric double layer moving in an infinite surrounding fluid. Smoluchowski obtained

$$v_e = \frac{\varepsilon_o \varepsilon_r \zeta E}{\mu}, \qquad (1)$$

in which v_e is the velocity of the particle in the stagnant fluid due to the applied electric field E, ε_o is the permittivity of free space, ε_r is the dielectric constant of the surrounding fluid, μ is the viscosity of the fluid, and ζ is the zeta potential. The zeta potential must be less than $|\pm 25|$ mV for eq 1 to be valid.

A measure of the thickness of the electric double layer is given by κ^{-1}, where κ is the Debye-Hückel parameter. The Debye-Hückel parameter is a function of the concentration of ionic species, C_i^{∞}, in the bulk solution, and the valence of the ions present, z_i, that is,

$$\kappa = \left(\frac{F^2 \sum_i C_i^{\infty} z_i^2}{\varepsilon_o \varepsilon_r RT} \right)^{1/2} \qquad (2)$$

Here F is Faraday's constant, R is the gas constant, and T is the absolute temperature. A thin electric double layer corresponds to large κa ($\kappa a > 100$), where *a* is the particle radius.

In an attempt to relax the restrictions in the Smoluchowski theory, Levine and Neale (16) obtained a complicated analytical solution for the electrophoretic velocity of a concentrated suspension of particles with an arbitrarily thick, but nonpolarizable electric double layer. To predict the electrical conductivity of a charged colloidal suspension, Johnson and Davis (17) developed a numerical solution for the electrophoretic velocity of a suspension of particles with arbitrarily thick, but non-overlapping, and nonpolarizable

electrical double layers. The distortion, or polarization, of the electric double layer causes a resistance to electrophoretic motion and is referred to as the relaxation effect. This effect has been shown to be small for small zeta potentials ($|\zeta| \leq 50$ mV) (17). Nonetheless, Kozak and Davis (18, 19) incorporated the relaxation effect and obtained a simpler analytical expression than that of Levine and Neale for the electrophoretic velocity of a suspension of particles. Their analyses was limited to moderately thick electric double layers ($\kappa a > 20$).

Despite the extensive number of electrophoretic experiments and the development of theoretical models for the electrophoresis of concentrated suspensions, there are relatively few published investigations that compare experimental clarification rates with theoretical predictions. The combined investigations are needed to validate theoretical models. This paper attempts to bridge this gap by reporting both experimental data and theoretical predictions for the clarification rate of a coal-washing effluent suspension and a colloidal TiO_2 suspension for various particle and/or electrolyte concentrations.

Colloid Properties

Since the unit cell model is based on a monodisperse and non-aggregating suspension of spherical colloidal particles, a colloidal suspension with similar characteristics must be used for experiments. Therefore, a 50 wt% colloidal suspension of polysiloxane coated TiO_2, with an average specific gravity of 3.87 g/ml, was obtained from Nanophase Technologies Corp. The volume average diameter of the particles was determined using a Horiba Model CAPA-500 centrifugal particle analyzer. By measuring the sedimentation rate by light transmission, the particle diameter was determined using the Stokes' centrifugal sedimentation equation. The sample suspension was diluted with biological grade water obtained from a Modulab Analytical Research Grade UF/Polishing

System (Continental Water Systems Corporation). The conductivity of this water was found to be 5.56 to 5.88 $\mu S\text{-}m^{-1}$, which is equivalent to an average concentration of 0.5 μM KCl for the data of Weast (20) based on a linear curve fit through the origin of a graph of conductivity versus concentration. The volume average diameter distribution of a sample that was not sonicated prior to analysis is shown in Figure 1. It can be observed from this figure that the suspension is only fairly monodisperse with an average diameter of 389 nm and a standard deviation of 287 nm. Nanophase Technologies Corp. claims that the majority of the 50 wt% suspension consists of primary particles with a diameter in the range of 25 to 51 nm. A comparison of the measured volume average size and the size of the primary particles indicates that some aggregation occurred. The results with the Horiba instrument were found to be repeatable, and the suspension was stable with respect to further aggregation. Although the suspension consisted of aggregates, it was assumed that the aggregates could be modeled as a spherical particle in order to compare results with theoretical models. Aggregation would also lower the density of an aggregated particle, thereby reducing the gravitational contribution of the forces exerted on a particle. The electrokinetic effects associated with the presence of the polysiloxane coating on the TiO_2 particles were neglected in the theoretical model. This assumption was verified by Ohshima (21) who showed that a polymer coated particle behaves similarly under electrophoresis to a solid particle if the thickness of the polymer shell, d^*, is much smaller than the radius of the particle, a. Based on TEM images obtained from Nanophase Technologies Corp., the thickness of the polymer coating is approximately 0.86 nm. If the volume average diameter of 389 nm is used, the ratio of d^*/a is 0.0044. According to Figure 2 in Ohshima (21) the ratio value of 0.0044 indicates that the polymer coating will have a negligible effect on the electrophoretic velocity of the particle.

The zeta potential of a dilute suspension of TiO_2 was measured using a Malvern Instruments Zetasizer 2c microelectrophoresis apparatus. The zeta potential was measured as a function of KCl concentration and pH with the results shown in Figures 2 and 3, respectively.

Electrophoretic clarification of the coal-washing wastewater obtained from the Centralia Mining Co. of Centralia, WA was also performed. The suspension had an initial pH of 8.2 and contained particles with a volume average diameter of 1.13 μm with a standard deviation of 1.08 μm and had the size distribution shown in Figure 4. The volume fraction of particles was 0.411%, which is equivalent to 0.493 wt% based on an average specific gravity of 1.2 g/ml. The water was analyzed for the cationic content to determine whether the particles had thin or thick electric double layers. The result of this analysis is shown in Table 4.1. It can be seen that the Na^+ cation is the primary species in solution. If it is assumed that the corresponding anion is Cl^-, then it can be determined that the particles have a thin double layer based on $\kappa a = 144$. The electrophoretic mobility of the particles was measured by diluting a sample and using a Rank Brothers Mark II microelectrophoresis apparatus. If the sample is sufficiently dilute, and the electrolyte concentration is high enough to produce thin electric double layers, then Smoluchowski's equation, eq 1, can be used to calculate the zeta potential of the particles (16, 22). For a suspension diluted to a volume fraction of $1*10^{-4}$ and an electrolyte (NaCl) concentration of 6 mM the average zeta potential was determined to be –41.9 mV.

According to Stokes' law, the terminal velocities of the particles in the TiO_2 suspension and coal-washing effluent are $1.56*10^{-7}$ m/s and $1.54*10^{-7}$ m/s, respectively. Based on this velocity, a suspension in the apparatus described below should clarify in less than 22 hours, however no observable clarification was observed over a period of 200 hours for either the TiO_2 or the coal-washing effluent suspension. The resistance to

gravitional sedimentation is due to Brownian motion and particle-particle interactions (hydrodynamic and electrostatic). As indicated above, the effective particle density of the TiO_2 aggregate is reduced from its primary particle density due to the void spaces, so it appears that the aggregate approached neutral buoyancy. Likewise, the particles in the coal-washing suspension are primarily clay particulates (80 wt%) which absorb water and approach neutral buoyancy. The reduced particle density was not accounted for in the Stokes' terminal velocity calculations reported above.

Experimental Apparatus

The electrophoretic apparatus used for the following experiments consisted of a square acrylic tank with inner dimensions of 14.2 x 14.2 x 3.2 cm. The bottom and top electrodes were made of a 0.64 cm thick carbon sheet with a cross section of 14.2 x 14.2 cm. The carbon electrodes were obtained from Graphite Sales, Inc. The electrodes were spaced 1.2 cm apart to provide a test volume of 242 ml. The power supply connected to the electrodes was a Hewlett-Packard 6218C DC supply.

The potential distribution was measured between the anode and cathode to determine the local electric field. The potential measurement was performed using the following procedure. A 16 gauge Teflon tube was filled with 3 wt% agar and 97 wt% KCl solution, the KCl concentration being the same as the test suspension in the apparatus. Upon heating, the presence of the agar caused a gel to form inside the Teflon tube. The gel was necessary in order to prevent mixing between the solution inside the tube and the suspension in the apparatus. To further prevent mixing between solutions, a porous glass frit was placed inside the end of the Teflon tube that was exposed to the colloidal suspension. The end of the tube, which contained the glass frit, was inserted through a 2 mm diameter hole drilled through the top electrode. The opposite end of the tube was placed in a jar containing a KCl solution having the same concentration as in the

colloidal suspension. A saturated calomel reference electrode (Fisher Scientific cat. no. 13-620-52) was also placed in the jar and connected to a Fluke multimeter (23 Series). The top electrode was connected to the same Fluke multimeter so that the potential difference between the location of the end of the Teflon tube and the top electrode (cathode for these experiments) could be measured. By traversing the flexible tube vertically and recording the potential every 3 mm, the potential distribution, and therefore the electric field, could be obtained.

As the particles moved due to electrophoresis, a sharp front formed between the colloidal suspension and the clarified solution above it. The location of the sharp front was measured by placing a ruler next to the apparatus and measuring the location of the front relative to the bottom electrode (anode).

Experiments

Experiments were conducted with either a TiO_2 suspension or the coal-washing effluent. The experiments conducted with the TiO_2 varied in initial volume fraction and initial electrolyte concentration. The volume fractions that were investigated were 0.001 and 0.003, which corresponds to a weight percent of 0.4 and 1.2, respectively. These volume fractions were obtained by diluting the original 50 wt% suspension with the biological grade water mentioned earlier. The electrolyte concentrations studied were 0.01 and 1 mM KCl.

The electrophoresis apparatus was filled with the suspension to be studied. The electric field was then applied as soon as any observable convective motion ceased. The experiments were performed under constant current conditions (0.58 mA or 28.8 mA/m^2). The maximum current density of 28.8 mA/m^2 was chosen because at higher current densities the generation of electrolysis gases became visible. Also, it was desired to keep

the production of H^+ and OH^- to a minimum since a change in the suspension pH changes the particles' zeta potential and increase the particles' susceptibility to additional aggregation.

To model the location of the clarification front, the following parameters that were varied must be specified: the volume fraction, α, the electrolyte concentration, C, and the electric field strength, E. The values of other parameters that must be specified, but were assumed to be constant for all experiments, are: dielectric constant of water, ε_r = 78.5, permittivity of free space, $\varepsilon_o = 8.854 \times 10^{-12}$ $C^2\text{-}N^{-1}\text{-}m^{-2}$, absolute temperature, T = 298 K, and viscosity of water, $\mu = 9.01 \times 10^{-4}$ $kg\text{-}m^{-1}\text{-}s^{-1}$. The particle diameter of 300 nm was used in the theoretical calculations for the TiO_2 suspensions since it can be seen from Figure 1 that the size distribution of the particles is centered on this diameter. Based on Figure 2, the average zeta potential for the TiO_2 particles of –66.7 mV was used in all theoretical calculations. Although the absolute value of the average zeta potential is greater than the limit of 50 mV for theories with nonpolarizable double layers, the neglect of the relaxation effect is assumed to have minimal influence on the electrophoretic velocity calculations. This is confirmed by observing the electrophoretic velocity results reported by Johnson and Davis (17). The particle diameter of 1.13 μm and average zeta potential of –41.9 mV were used for all calculations related to the coal-washing suspension.

Electric Field Distribution for the TiO_2 Experiments

Table 2 shows the electric field strength as a function of location and time, along with the location of the clarification front over time, for a TiO_2 suspension with an initial particle concentration of 1.2 wt% and electrolyte concentration of 0.01 mM KCl. By observing the position of the front and the electric field distribution below the front, it can

be seen that the average electric field is 0.67 V/m. Due to the conductivity of the colloidal suspension and the low current densities, the accuracy of the measured potential differences in the suspension is limited by the accuracy of the Fluke multimeter. Despite the large error that occurs by operating at this limit it is felt that the number of measurements taken and the consistent reading of 0.67 V/m within the suspension justifies the use of this value for theoretical computations for this particular suspension. The same reasoning was used for the other experimental suspensions for the numerical value of the electric field strength. Sauer and Davis (10) used a similar method to determine the electric field distribution within an electrophoretic apparatus, but their results indicated a dramatic change in the strength of the electric field near the sharp clarification front. This phenomenon was not observed in the current apparatus, so it is likely that their results were due to edge effects associate with their thin electrophoresis cell.

Experiments with a 0.4 wt% TiO_2 Suspension

The experimental data for the location of the front as a function of time for a colloidal suspension with an initial particle volume fraction of 0.001 (0.4 wt%) and an initial electrolyte concentration of 0.01 mM KCl ($\kappa a = 1.56$) is shown in Figure 5. The initial conductivity of the suspension was 52.9 mS-m^{-1} and the average electric field was measured to be 1.0 V/m within the colloidal suspension. Also shown in Figure 5 are the theoretical predictions for the clarification front as predicted by Smoluchowski's equation (eq 1), Levine and Neale's model (16), and our numerical model (17). The theory of Kozak and Davis (19) was not used since it is not valid for $\kappa a < 20$. It can be seen that our numerical model and that of Levine and Neale agree with the measured clarification front, and the Smoluchowski equation greatly overpredicts the movement of the front.

The deviation between the experimental data and the theoretical predictions for times greater than 72 hours is due to the fact that the theoretical models are based on a suspension of infinite depth. In a finite volume and/or geometry upflow of water from the consolidated layer on the bottom electrode opposes the motion induced by the electric field. The hypothesis that the deviation is due to the characteristics of the apparatus is supported by the fact that the final location of the front is independent of the suspension characteristics (e.g. particle or electrolyte concentration).

The experimental data and theoretical predictions for a 0.4 wt% suspension having an initial electrolyte concentration of 1 mM KCl ($\kappa a = 15.6$) are shown in Figure 6. The average electric field strength was 0.67 V/m in this colloidal suspension compared to 1.0 V/m for the previous experiment. This decrease is due to the higher electrolyte concentration and the corresponding increase in the electrical conductivity to 77.9mS-m^{-1}. Our numerical model, Levine and Neale's result, and the Smoluchowski equation yield similar results for the location of the front for the thin double layer encountered in this case. Note that the front velocity increases significantly for times greater than 45 hours. Since this velocity is greater than Smoluchowski's theoretical maximum electrophoretic velocity, it is likely that significant aggregation occurred, leading to gravitational sedimentation. Additional aggregation is due to the increase in the initial electrolyte concentration, which leads to thinner double layers and an increase in the probability of particle-particle collisions. Since the theoretical models do not account for gravitational sedimentation, the predictions were not extended into this region.

Experiments with a 1.2 wt% TiO_2 Suspension

The experiments were repeated with an initial particle concentration three times that of the previous case. Figure 7 displays the experimental data and the theoretical

predictions for a 1.2wt% suspension with 0.01 mM KCl ($\kappa a = 1.56$). The average electric field strength was 0.67 V/m, which is lower than that obtained from the experiment with 0.4 wt% TiO_2 and 0.01 mM KCl. This is due to the increase in the overall electrical conductivity to 114.9 $mS\text{-}m^{-1}$ with the addition of more particles. It can be seen that our numerical model provides a significant improvement in modeling the location of the front compared to the theory of Levine and Neale. Also, it is observed that the front stabilizes between 60 and 90 hours. This is possibly due to electric double layer polarization caused by the production and diffusion of H^+ and OH^- at the electrodes. The polarization of the double layer is a stabilizing effect against electrophoretic motion. After 90 hours the front again moves toward the anode. This is probably due to the continued production of H^+ and OH^- ions, which, besides polarizing and distorting the double layer, causes the double layer to become compressed and leads to increased particle-particle collisions, aggregation, and gravitational sedimentation. The production of ions due to electrolysis resulted in a decrease in pH of the overall suspension from an initial value of 8.9 to a final value of 5.0.

Figure 8 displays the experimental data and the theoretical predictions for a suspension with 1.2 wt% particles, but with an increased electrolyte content equal to 1mM KCl ($\kappa a = 15.6$). The initial conductivity of the suspension was 135.2 $mS\text{-}m^{-1}$ and the average electric field was found to be 0.33 V/m within the colloidal suspension. Again, when the electrolyte concentration is not low, our numerical model offers no significant improvement in the ability to predict the location of the front. The result of our model and that of Levine and Neale overlap on the figure. Also, the trend in the clarification position as a function of time is similar to the experiment with 1.2 wt% TiO_2 and 0.01 mM KCl. The front stabilized against further clarification at 7 mm from the

anode for several hours, and then aggregation occurred leading to gravitational sedimentation.

Coal-Washing Effluent

The electric field as a function of position and time, along with the location of the front over time, was measured for the coal-washing suspension. Due to the high conductivity of the colloidal suspension (437 $mS\text{-}m^{-1}$) and the low current densities, the measured potential differences in the suspension were small. The average field strength over time, based on the probe measurements, varied between 0.67 V/m in the upper 3 mm near the cathode and 0.11 V/m in the lower 9 mm. Table 3 lists only the average electric field strength over these two regions. The larger average electric field near the cathode is due to the overpotential between the electrode and the adjacent fluid associated with electrolysis and does not represent the effective local electric field.

The experimental data for the position of the clarification front is shown in Figure 9. Also shown in the figure are the theoretical predictions for the clarification front for times less than 110 hours as predicted by our numerical model using the electric field strengths 0.67 V/m and 0.11 V/m. Predictions based on Smoluchowski's equation and Levine and Neale's model are not shown since our model provides only a slight deviation from their results due to the low zeta potential of the particles and the high electrolyte content of the suspension. Our model calculations were based on a single z-z electrolyte ($z = z_+ = -z_-$) with a concentration of 6 mM (assuming Cl^- as the anion) since the concentration of Na^+ in solution is the dominate ionic species and was measured to be 350 mg/L. The model does not incorporate double layer distortion, which would occur for any Na^+-anion combination. It has been shown that double layer distortion will have

a negligible effect on the electrophoretic mobility for a suspension with thin double layers ($\kappa a = 144$) and with a volume fraction of 0.411% (17).

When a field strength of 0.67 V/m is used, the model greatly overpredicts the movement of the front even though the front was located within 3 mm of the cathode. This suggests that the effective electric field was lower than 0.67 V/m. When the electric field strength of 0.11 V/m is used in the theoretical model, the predictions are in reasonable agreement with the experimental data. Thus, it can be concluded that the potential measurements near the cathode incorporated an electrochemical effect, which cannot be resolved with the current potential measuring method. For $100 < t < 175$ hours, it appears that particle-particle aggregation occurred, for the velocity of the front increased. For $t > 175$ hours clarification ceased. This could be due to the change in the water chemistry due to the production of ions from electrolysis reactions (final pH = 4.30) and/or due to interparticle effects between coal and clay particles that stabilize the suspension against further aggregation, electrophoretic movement, or gravitational sedimentation.

Comments

The clarification of concentrated colloidal suspensions by electrophoresis is complicated by particle-particle interactions that affect the drag force on the particle and electrochemical reactions at the electrodes. The production of ions at the electrodes alters the thickness of the electric double layer and the pH of the solution. A change in pH generally affects the zeta potential. All of these phenomena occur simultaneously during the electrokinetic separation process. A unit cell model appears to take into account hydrodynamic interactions adequately. If the local electric field is measured and used in

the model, the velocity of the well-defined front that forms between the clear solution and the sedimenting particles is predicted satisfactorily.

A more complete prediction that can be used to scale up laboratory experiments needs to take into account the electric potential in the vicinity of the electrodes, the upflow associated with the compressed layers that have sedimented, the effect of pH on the zeta potential and the ion production at the electrodes.

Acknowledgments

The authors wish to thank the Department of Energy (DE-FG22-95PC95209) for the financial support of this research.

Literature Cited

(1) Grant, C. S.; Matteson, M. J.; Clayfield, E. J. *Sep. Sci. Technol.* **1991**, 26, 773-802.

(2) Reuss, F. F. *Mem. Soc. Imp. Naturalistes Moscou* **1809**, 2, 3227.

(3) Tiselius, A. *Trans. Faraday. Soc.* **1937**, 33, 524.

(4) Casagrande, L. U.S. Patent No. 2,099,3281, 1937.

(5) Sprute, R. H.; Kelsh, D. J. *Bur. Mines Rep. Invest.* **1982**, No. 8666, 32 pp.

(6) Stanczyk, M. H.; Feld, I. L. *Bur. Mines Rep. Invest.* **1964**, No. 6451, .

(7) Lockhart, N. C. *Colloids Surf.* **1983**, 6, 229-251.

(8) Wilmans, W.; Van Deventer, J. S. J. *J. S. Afr. Inst. Min. Metall.* **1987**, 87, 41-51.

(9) Yoshida, H.; Shinkawa, T.; Yukawa, H. *J. Chem. Eng. Jpn.* **1985**, 18, 337-342.

(10) Sauer, J. E.; Davis, E. J. *Environ. Sci. Technol.* **1994**, 28, 737-45.

(11) Johnson, T.; Davis, E. J. *Environ. Sci. Technol.* **1999**, 33, 1250-55.

(12) Shih, Y. T.; Gidaspow, D.; Wasan, D. T. *Colloids Surf.* **1986**, 21, 393-429.

(13) Lee, C.; Gidaspow, D.; Wasan, D. T. *Paper presented at the International Powder and Solids Handling and Processing Conference*, Philadelphia, PA, 1979.

(14) Matsumoto, K.; Kutowy, O.; Capes, C. E. *Powder Technol.* **1981**, 28, 205-15.

(15) Smoluchowski, M. *Handbuch der Electrizitat und des Magnetismus, Vol. II*; Barth: Leipzig, 1921, p 366.

(16) Levine, S; Neale, G. H. *J. Colloid Interface Sci.*, **1974**, 47, 520-29.

(17) Johnson, T.; Davis, E. J. *J. Colloid Interface Sci.* **1999**, in press.

(18) Kozak, M. W.; Davis, E. J. *J. Colloid Interface Sci.* **1989**, 127, 497-510.

(19) Kozak, M. W.; Davis, E. J. *J. Colloid Interface Sci.* **1989**, 129, 166-74.

(20) Weast, R. C. *Handbook of Chemistry and Physics, 53rd Ed.*, CRC Press, Ohio, 1972.

(21) Ohshima, H. *J. Colloid Interface Sci.*, **1994**, 163, 474-83.

(22) O'Brien, R. W., White, L. R. *J. Chem. Soc. Faraday Trans.*, **1978**, 74, 1607-26.

Table 1 Cationic content of the coal-washing suspension obtained from the Centralia Mining Co.

Cation	Ca^{+2}	Mg^{+2}	Na^{+1}	Sr^{+2}
Concentration, mg/L	11.4	3.2	350.1	0.39

Table 2 The electric field (V/m) in the suspension as a function of time and the location of the clarification front for an initial TiO_2 particle concentration of 1.2 wt% and an initial electrolyte concentration of 0.01 mM KCl.

Distance From Anode, mm	Time, hr							
	0	6	18	30	52.5	79	102	
9 - 12	0.67	1.0	1.0	1.33	1.0	1.0	0.67	
6 - 9	0.67	0.67	0.33	0.67	0.67	0.67	0.67	
3 - 6	0.67	0.67	0.67	0.33	0.33	0.67	0.67	
0 - 3	0.67	0.67	1.0	1.0	0.67	0.67	0.33	
	12.0	11.0	10.7	9.9	8.3	7.0	5.9	Front Location, mm

Table 3 The electric field (V/m) in the suspension as a function of time and the location of the clarification front for the experiment with the coal-washing effluent.

Distance From Anode, mm	Time, hr							
	3	30.5	60.3	98.8	132	167	190	
9 - 12	0.33	0.67	0.67	0.67	0.33	0.67	0.67	
0 – 9	0.11	0.11	0.11	0.11	0.11	0.11	0.11	
	11.9	11.7	11.0	10.5	9.25	7.5	7.25	Front Location, mm

Figure Captions

Figure 1 Size distribution of the polysiloxane coated TiO_2 particles.

Figure 2 Zeta potential of polysiloxane coated TiO_2 as a function of KCl concentration.

Figure 3 Zeta potential of polysiloxane coated TiO_2 as a function of pH.

Figure 4 Size distribution of the particles in the coal-washing effluent.

Figure 5 Clarification front as a function of time for a colloidal suspension with an initial particle volume fraction of 0.001 (0.4 wt%) and an initial electrolyte concentration of 0.01 mM KCl.

Figure 6 Clarification front as a function of time for a colloidal suspension with an initial particle volume fraction of 0.001 (0.4 wt%) and an initial electrolyte concentration of 1.0 mM KCl.

Figure 7 Clarification front as a function of time for a colloidal suspension with an initial particle volume fraction of 0.003 (1.2 wt%) and an initial electrolyte concentration of 0.01 mM KCl.

Figure 8 Clarification front as a function of time for a colloidal suspension with an initial particle volume fraction of 0.003 (1.2 wt%) and an initial electrolyte concentration of 1 mM KCl. The results of Levine and Neale overlap our model results.

Figure 9 Clarification front as a function of time for the coal-washing suspension. Theoretical predictions based on a particle volume fraction of 0.411% and an initial electrolyte concentration of 6 mM NaCl.

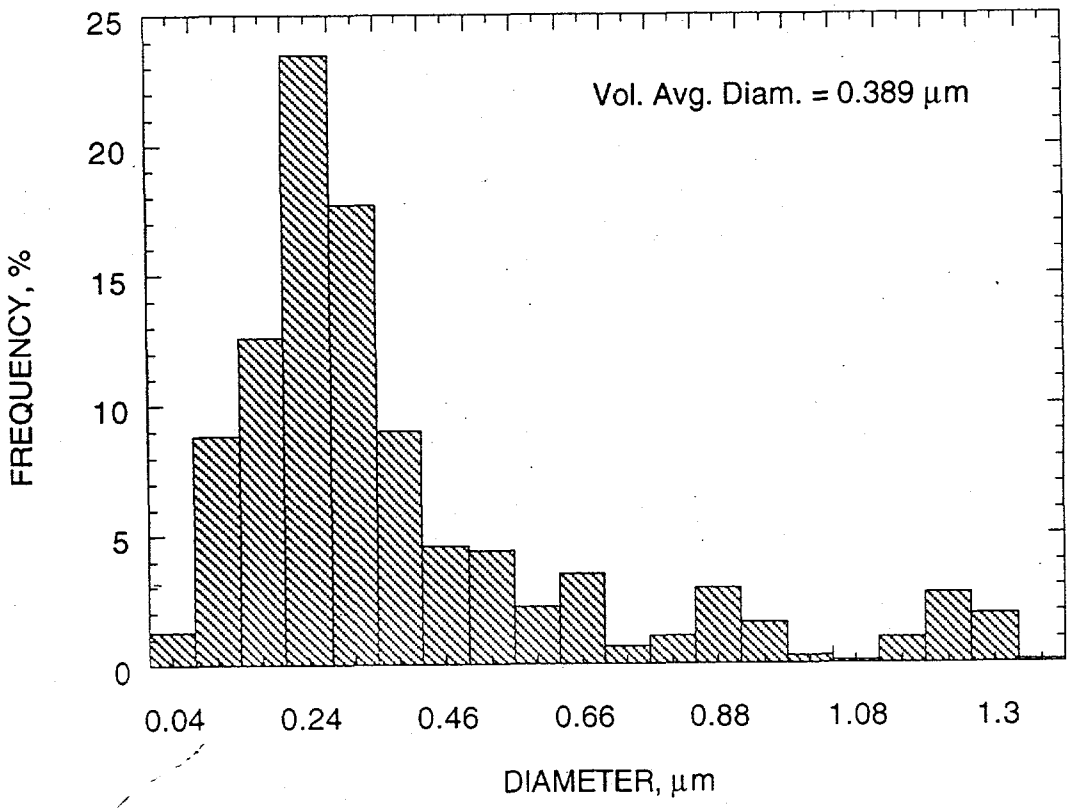
Vol. Avg. Diam. = 0.389 µm
FREQUENCY, %
25
20
15
10
5
0
0.04
0.24
0.46
0.66
0.88
1.08
1.3
DIAMETER, µm

Figure 1.

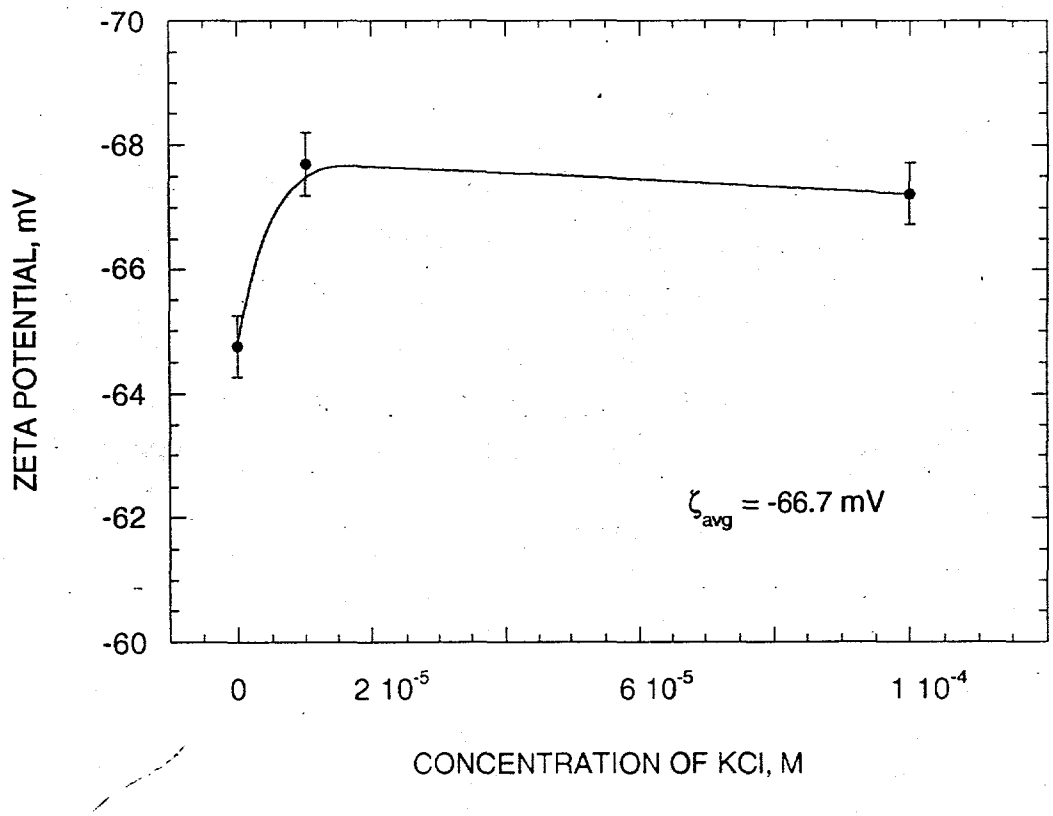
-70
-68
-66
-64
-62
-60
ZETA POTENTIAL, mV
0
2 10-5
6 10-5
1 10-4
CONCENTRATION OF KCl, M
ζavg = -66.7 mV

Figure 2.

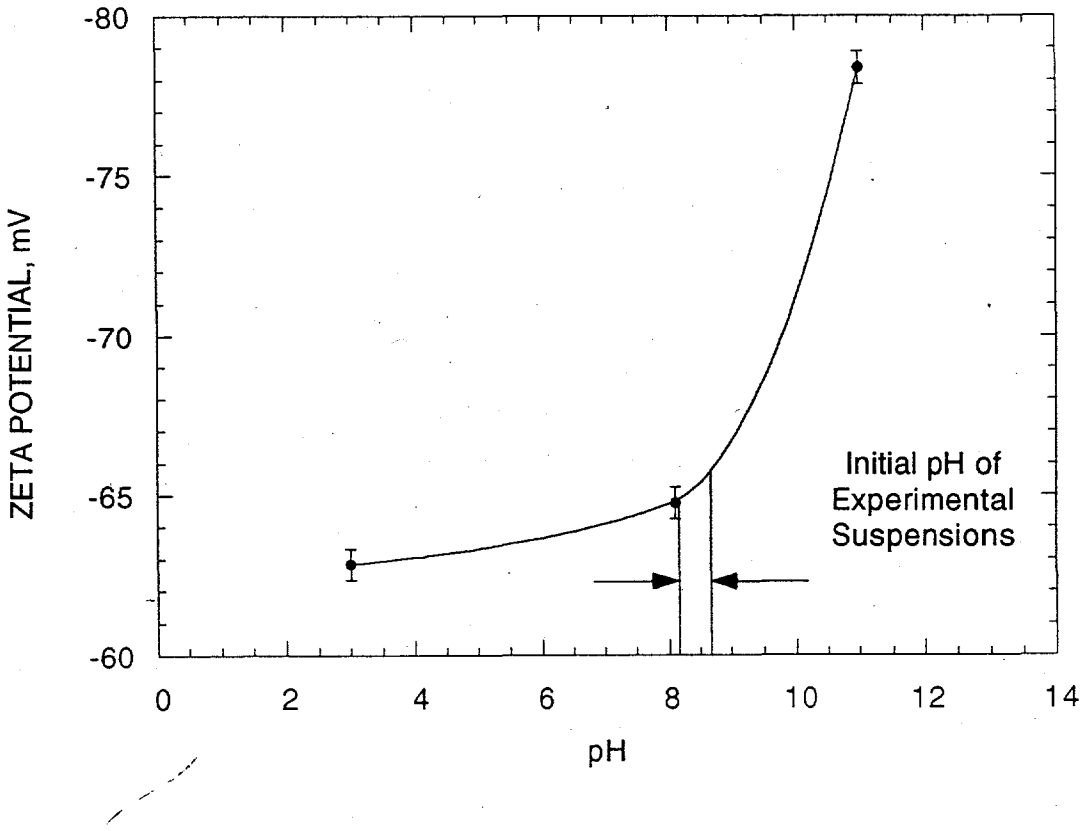
-80
-75
-70
-65
-60
ZETA POTENTIAL, mV
0
2
4
6
8
10
12
14
pH
Initial pH of
Experimental
Suspensions

Figure 3.

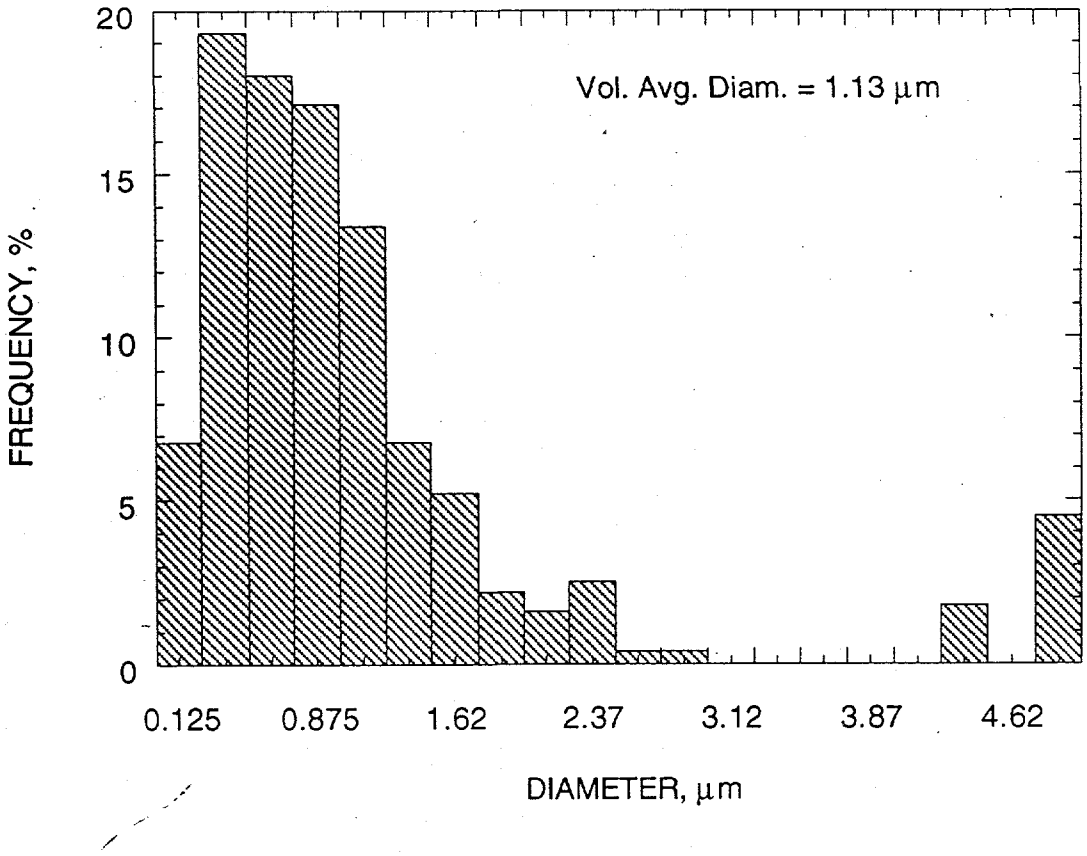
20
15
10
5
0
FREQUENCY, %
Vol. Avg. Diam. = 1.13 µm
0.125
0.875
1.62
2.37
3.12
3.87
4.62
DIAMETER, µm

Figure 4.

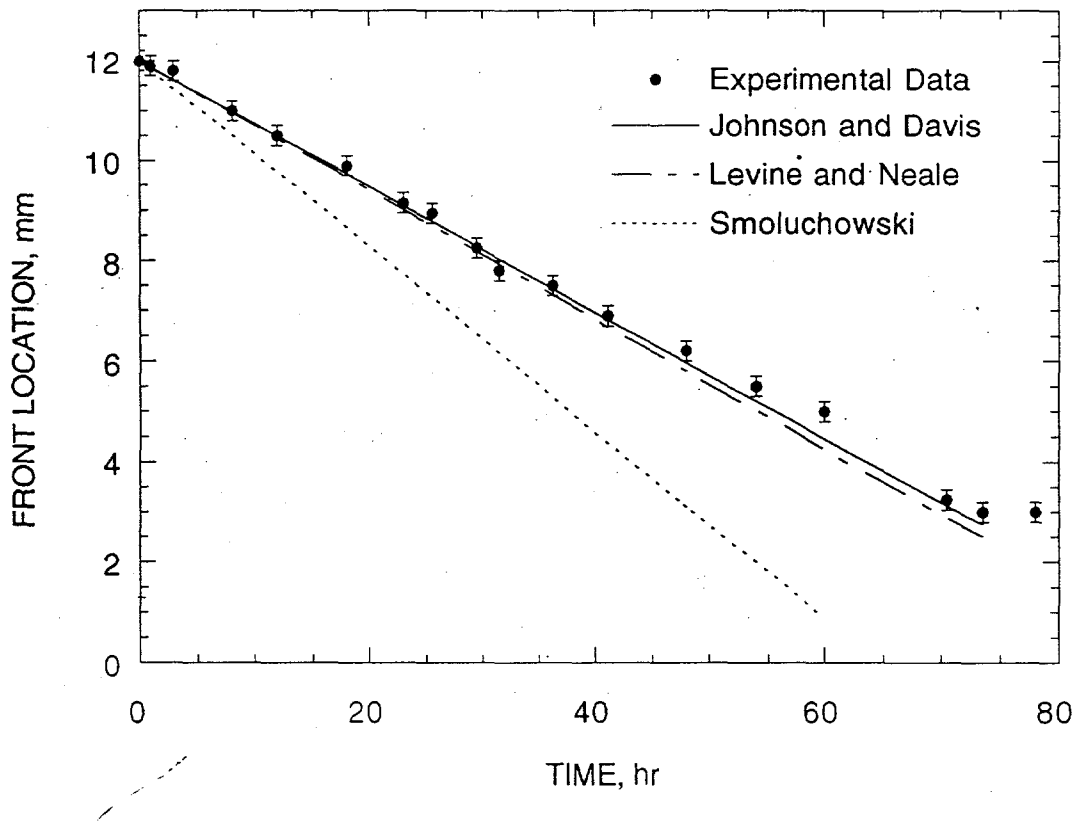
Experimental Data
Johnson and Davis
Levine and Neale
Smoluchowski
FRONT LOCATION, mm
TIME, hr
0
2
4
6
8
10
12
0
20
40
60
80

Figure 5.

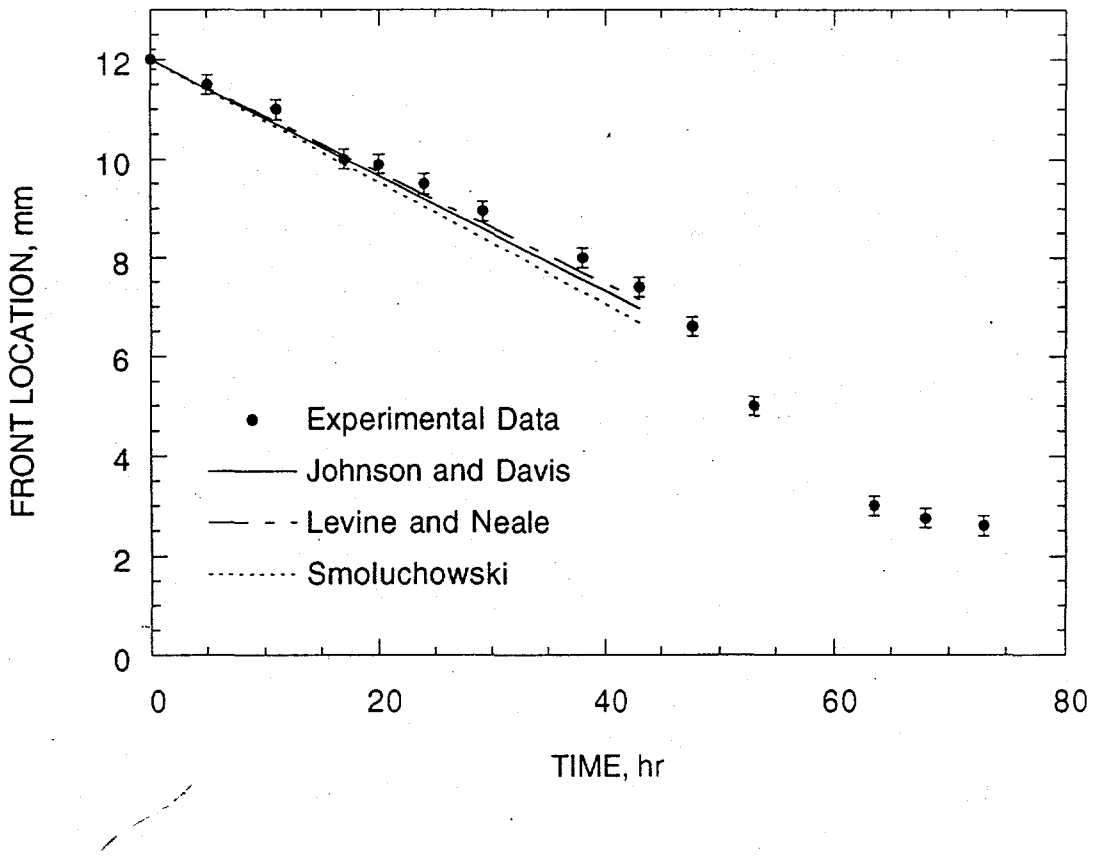
FRONT LOCATION, mm
TIME, hr
0
2
4
6
8
10
12
0
20
40
60
80
Experimental Data
Johnson and Davis
Levine and Neale
Smoluchowski

Figure 6.

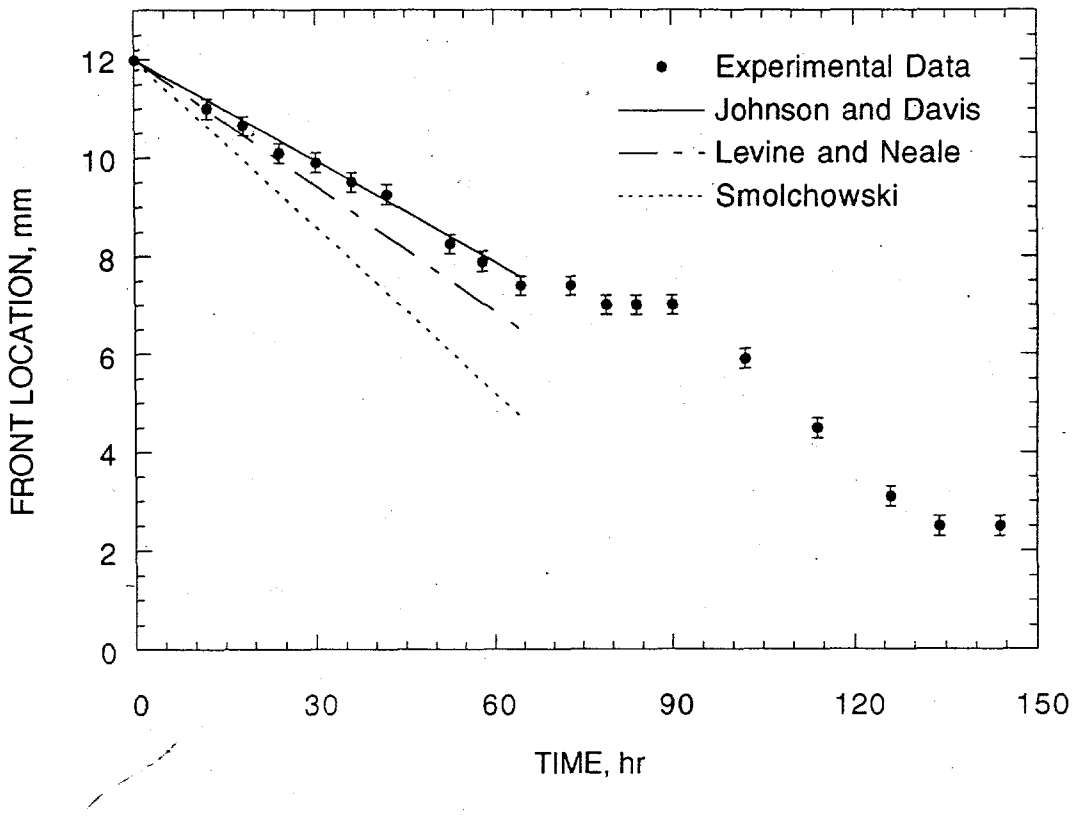
Experimental Data
Johnson and Davis
Levine and Neale
Smolchowski
FRONT LOCATION, mm
TIME, hr
0
2
4
6
8
10
12
0
30
60
90
120
150

Figure 7.

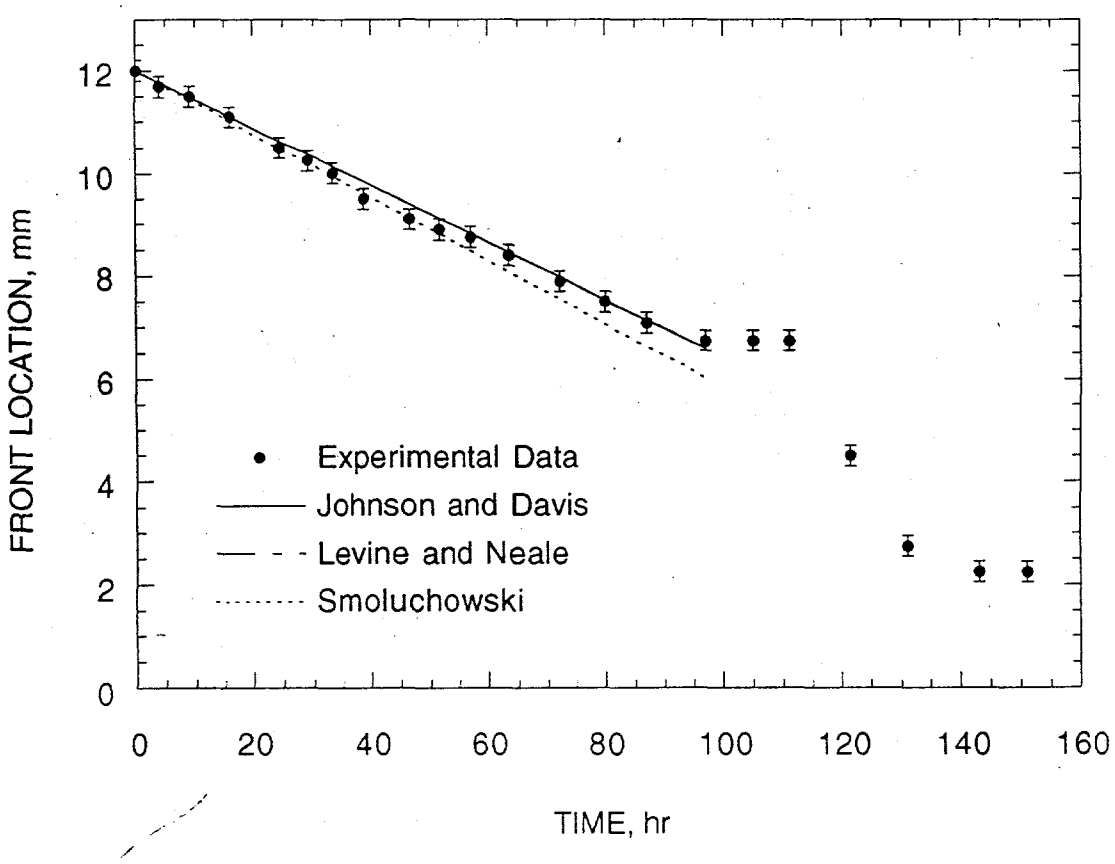
FRONT LOCATION, mm
TIME, hr
0
2
4
6
8
10
12
0
20
40
60
80
100
120
140
160
Experimental Data
Johnson and Davis
Levine and Neale
Smoluchowski

Figure 8.

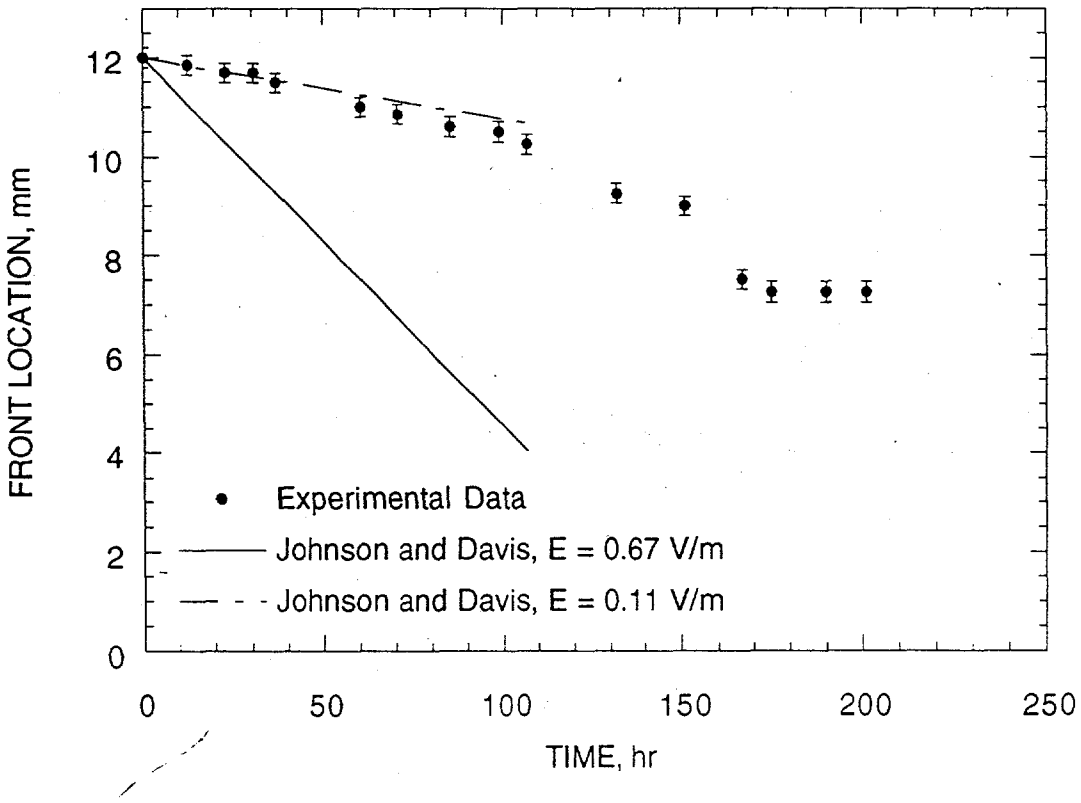
FRONT LOCATION, mm
TIME, hr
0
2
4
6
8
10
12
0
50
100
150
200
250
Experimental Data
Johnson and Davis, E = 0.67 V/m
Johnson and Davis, E = 0.11 V/m

Figure 9.